

Lecture 3: Medical Images: Classification (Part 2), Segmentation

Announcements

- A0 due tomorrow
- A1 will be released tomorrow, due in 2 weeks (Tue 10/18)
 - You will need to download several datasets to do the assignment. Make sure to start early!
 - 3 parts:
 - Medical image classification
 - Medical image segmentation in 2D
 - Medical image segmentation in 3D, with semi-supervised learning
- Tensorflow Review Session this Fri 1:30pm, helpful for A1

Announcements - Course project

- Start thinking about your course project
 - Project proposal due Fri 10/21
 - See <http://biods220.stanford.edu/finalproject.html> for project components and requirements
 - **Released on Ed (#35): some project resources (open source datasets, and ideas curated from the Stanford Med School and broader community)**
 - Contributed project ideas are not vetted, you need to do your due diligence
 - Is the dataset easily accessible and well suited to machine learning? Access and play with the data before the project proposal, and make sure you can use GPU compute.
 - Is there a clearly defined task for which you can apply deep learning?
 - Can you evaluate your method?
 - Will need to answer these questions in the project proposal
 - If you are not sure, come to any of the teaching staff office hours. We are happy to discuss your project with you!

Announcements - Course project

- Preview of graded components:
 - Proposal: Due Fri 10/21.
 - Milestone: Due Fri 11/18.
 - TA project advising sessions: after the milestone, details TBD.
 - Final project poster session: In person, during the final exam period for this course (Wed 12/14, 3:30-6:30pm)
 - Final report due: Fri 12/16.

Google dataset search

datasetsearch.research.google.com

The screenshot shows the Google Dataset Search interface. At the top, the Google logo is on the left, and a search bar contains the text "lung nodule detection". Below the search bar are filters for "Updated Date", "Download Format", "Usage Rights", and "Free". The search results show "100+ datasets found". The top result is from Kaggle, titled "Lung Nodule Malignancy" with the subtitle "From suspicious nodules to diagnosis". It includes a link to "Explore at Kaggle" and mentions that 218 scholarly articles cite this dataset. Below this are sections for "Dataset updated", "Authors" (Kevin Mader), "License", and "Available download formats from providers". A "Description" section follows, starting with "Context" and a paragraph about the DataScienceBowl project.

Google

lung nodule detection

Updated Date Download Format Usage Rights Free

100+ datasets found

kaggle Lung Nodule Malignancy
www.kaggle.com
Updated Sep 21, 2017

A LUng Nodule Analysis (LUNA16)
All Images
academicorrents.com
Updated Jul 15, 2018

F Detection of artificial pulmonary lung nodules in...
figshare.com
Updated Jan 4, 2018

R Applying Ant Colony Optimization algorithms and...
www.researchgate.net
Updated Dec 6, 2013

kaggle

Lung Nodule Malignancy
From suspicious nodules to diagnosis

Explore at Kaggle

218 scholarly articles cite this dataset (View in Google Scholar)

Dataset updated Sep 21, 2017

Authors
Kevin Mader

License
Other (specified in description)

Available download formats from providers
hdf5 (64618370 bytes), csv (65813 bytes), zip (175233019 bytes), tif (110548836 bytes)

Description
Context

The DataScienceBowl covered the whole process of diagnosing lung cancer and I am to make the individual steps more clear. After segmenting lungs and ident malignant or benign.

Announcements - Review sessions

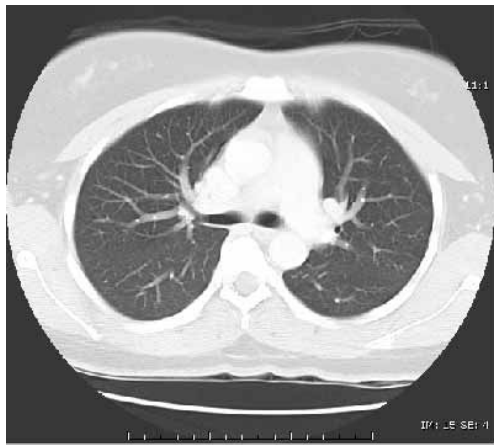
- Was in Alway M112 last Friday, but will be in **Alway M106** moving forward
- Due to incorrect location on Friday, did not get session recording
- Last year's video recording of the material (almost identical, slightly re-arranged) is on Canvas (see pinned Ed post). Was a lecture last year, spun out into review session this year based on student feedback.
- Apparently the university may have also recorded in M112 on Friday, they are working on getting that recording out so it may also be shared.

Last time: Deep learning models for image classification

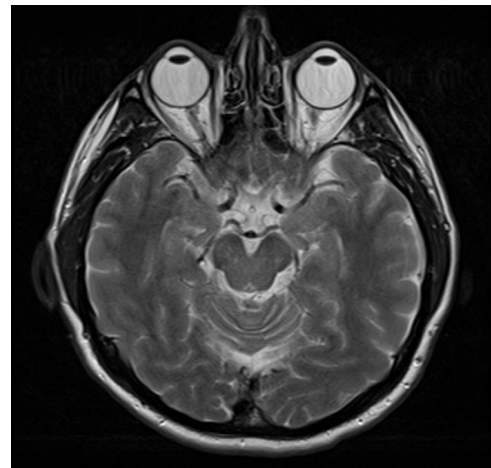
E.g.:



X-rays (invented 1895).



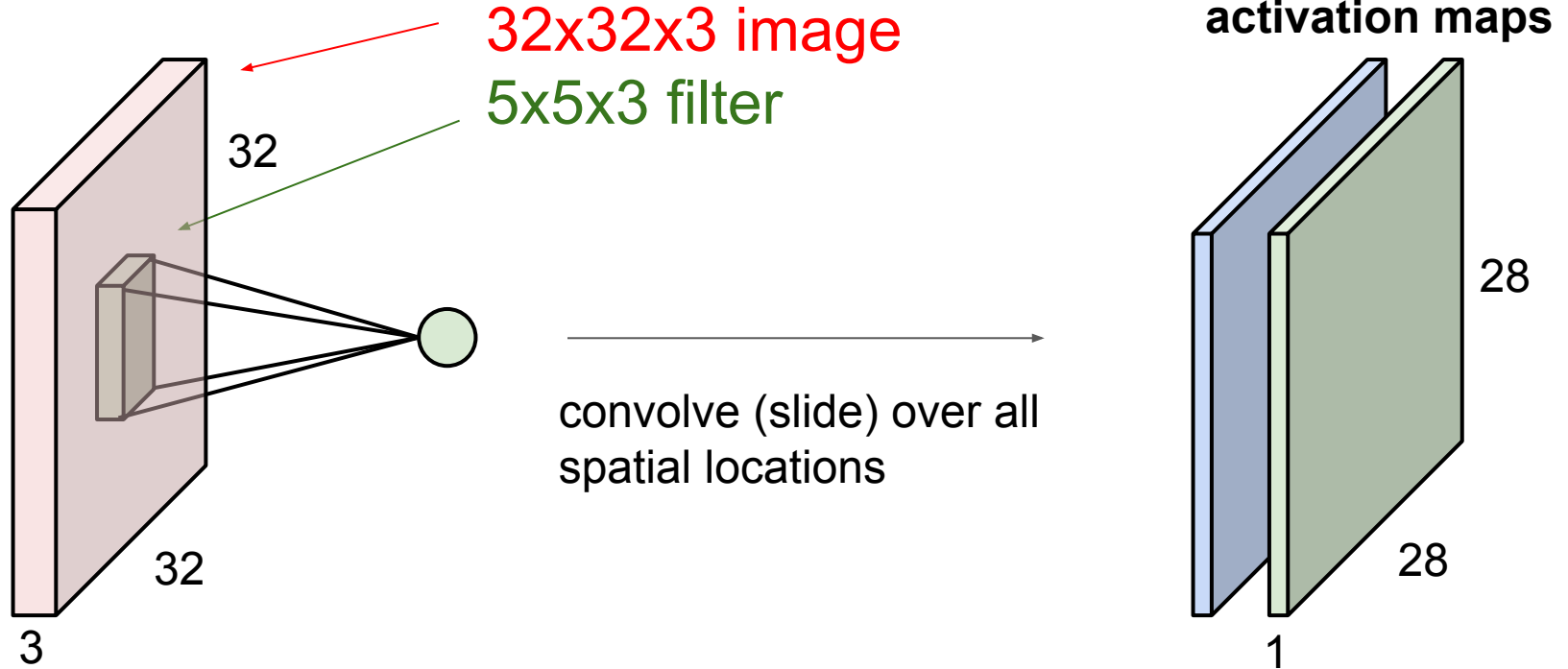
CT (invented 1972).



MRI (invented 1977).

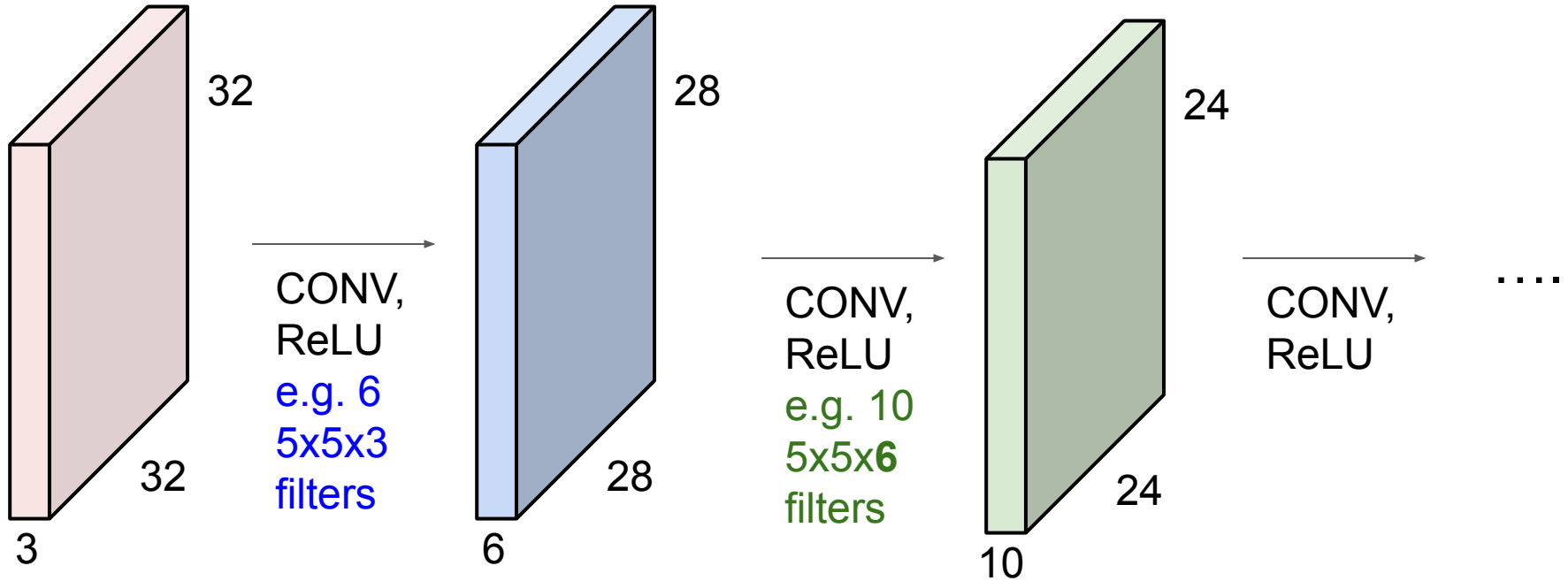
consider a second, **green** filter

Convolutional layer



Slide credit: CS231n

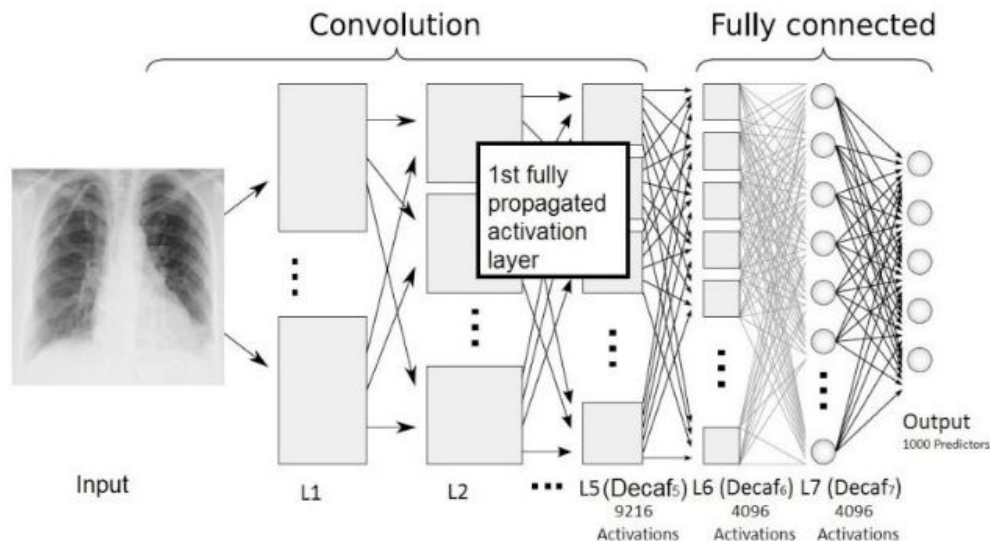
Preview: ConvNet (or CNN) is a sequence of Convolution Layers, interspersed with activation functions



Slide credit: CS231n

Bar et al. 2015

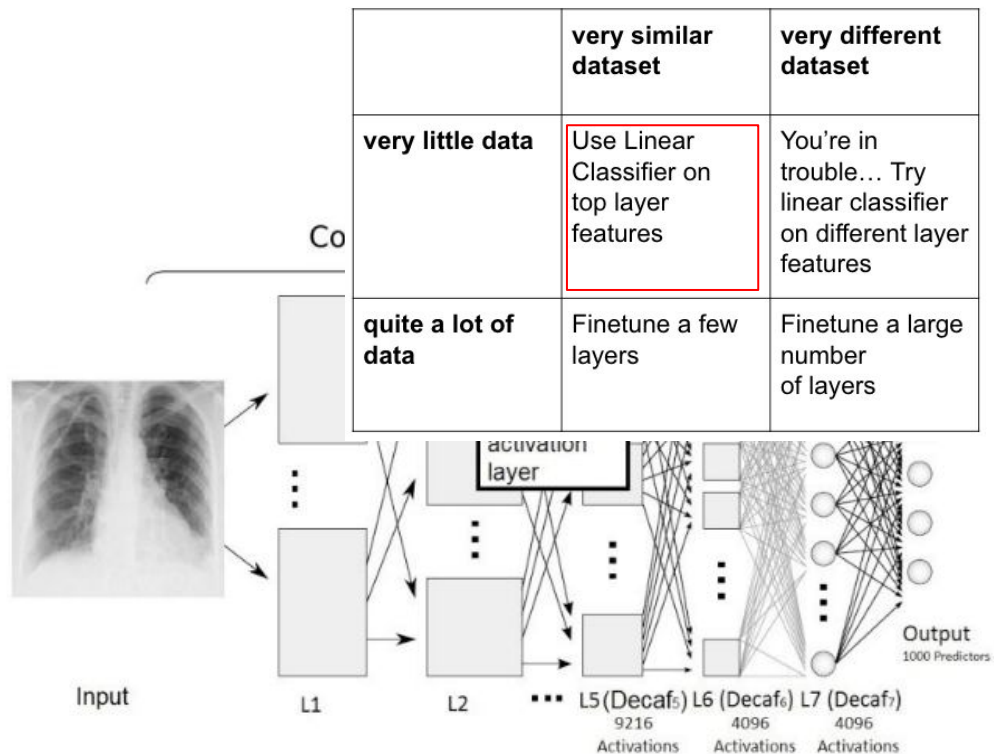
- Did not train a deep learning model on the medical data
- Instead, extracted features from an AlexNet trained on ImageNet
 - 5th, 6th, and 7th layers
- Used extracted features with an SVM classifier
- Performed zero-mean unit-variance normalization of all features
- Evaluated combination with other hand-crafted image features



Bar et al. Deep learning with non-medical training used for chest pathology identification. SPIE, 2015.

Bar et al. 2015

- Did not train a deep learning model on the medical data
- Instead, extracted features from an AlexNet trained on ImageNet
 - 5th, 6th, and 7th layers
- Used extracted features with an SVM classifier
- Performed zero-mean unit-variance normalization of all features
- Evaluated combination with other hand-crafted image features



Bar et al. Deep learning with non-medical training used for chest pathology identification. SPIE, 2015.

Bar et al. 2015

Table 1. Right Pleural Effusion Condition.

	Low Level		High Level	Deep			Fusion
	LBP	GIST	PiCoDes	Decaf L5	Decaf L6	Decaf L7	PiCoDes+Decaf L5
Sensitivity	0.71	0.79	0.79	0.93	0.86	0.86	0.93
Specificity	0.77	0.92	0.91	0.84	0.86	0.80	0.84
AUC	0.75	0.93	0.91	0.92	0.91	0.84	0.93

Table 2. Healthy vs. Pathology.

	Low Level		High Level	Deep			Fusion
	LBP	GIST	PiCoDes	Decaf L5	Decaf L6	Decaf L7	PiCoDes+Decaf L5
Sensitivity	0.65	0.68	0.59	0.73	0.89	0.76	0.81
Specificity	0.61	0.66	0.79	0.80	0.64	0.64	0.79
AUC	0.63	0.72	0.72	0.78	0.79	0.72	0.79

Table 3. Enlarged Heart Condition.

	Low Level		High Level	Deep			Fusion
	LBP	GIST	PiCoDes	Decaf L5	Decaf L6	Decaf L7	PiCoDes+Decaf L5
Sensitivity	0.75	0.79	0.79	0.88	0.79	0.79	0.83
Specificity	0.78	0.81	0.84	0.78	0.88	0.77	0.84
AUC	0.80	0.82	0.87	0.87	0.84	0.79	0.89

Bar et al. Deep learning with non-medical training used for chest pathology identification. SPIE, 2015.

Bar et al. 2015

Q: How might we interpret the AUC vs. CNN feature trends?

Table 1. Right Pleural Effusion Condition.

	Low Level		High Level	Deep			Fusion
	LBP	GIST	PiCoDes	Decaf L5	Decaf L6	Decaf L7	PiCoDes+Decaf L5
Sensitivity	0.71	0.79	0.79	0.93	0.86	0.86	0.93
Specificity	0.77	0.92	0.91	0.84	0.86	0.80	0.84
AUC	0.75	0.93	0.91	0.92	0.91	0.84	0.93

Table 2. Healthy vs. Pathology.

	Low Level		High Level	Deep			Fusion
	LBP	GIST	PiCoDes	Decaf L5	Decaf L6	Decaf L7	PiCoDes+Decaf L5
Sensitivity	0.65	0.68	0.59	0.73	0.89	0.76	0.81
Specificity	0.61	0.66	0.79	0.80	0.64	0.64	0.79
AUC	0.63	0.72	0.72	0.78	0.79	0.72	0.79

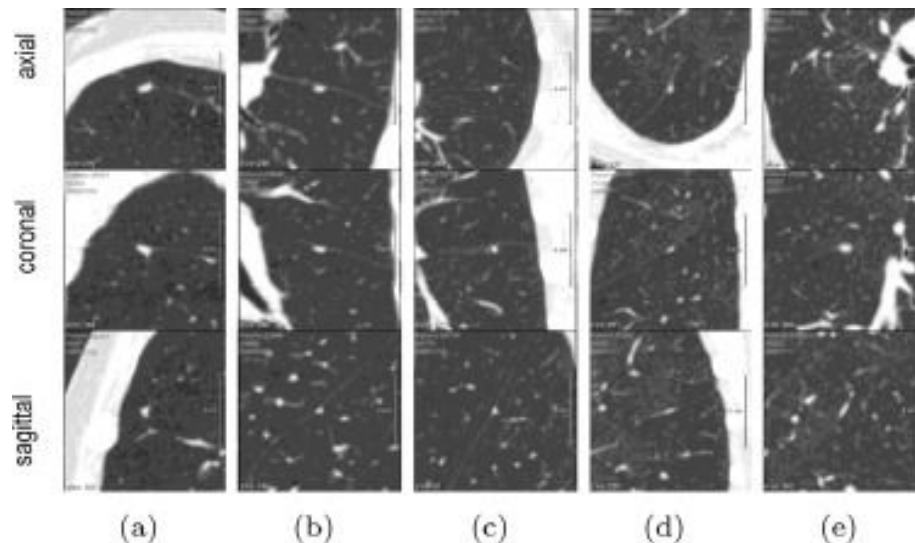
Table 3. Enlarged Heart Condition.

	Low Level		High Level	Deep			Fusion
	LBP	GIST	PiCoDes	Decaf L5	Decaf L6	Decaf L7	PiCoDes+Decaf L5
Sensitivity	0.75	0.79	0.79	0.88	0.79	0.79	0.83
Specificity	0.78	0.81	0.84	0.78	0.88	0.77	0.84
AUC	0.80	0.82	0.87	0.87	0.84	0.79	0.89

Bar et al. Deep learning with non-medical training used for chest pathology identification. SPIE, 2015.

Ciampi et al. 2015

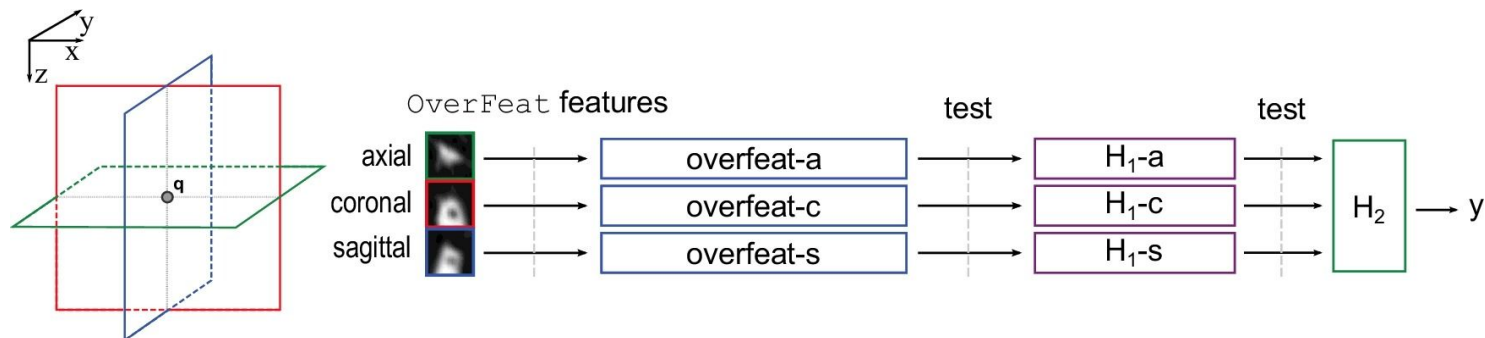
- Task: classification of lung nodules in **3D CT scans** as peri-fissural nodules (PFN, likely to be benign) or not
- Dataset: 568 nodules from 1729 scans at a single institution. (65 typical PFNs, 19 atypical PFNs, 484 non-PFNs).
- Data pre-processing: prescaling from CT hounsfield units (HU) into $[0,255]$. Replicate 3x across R,G,B channels to match input dimensions of ImageNet-trained CNNs.



Ciampi et al. Automatic classification of pulmonary peri-fissural nodules in computed tomography using an ensemble of 2D views and a convolutional neural network out-of-the-box. *Medical Image Analysis*, 2015.

Ciompi et al. 2015

- Also extracted features from a deep learning model trained on ImageNet
 - Overfeat feature extractor (similar to AlexNet, but trained using additional losses for localization and detection)
 - To capture 3D information, extracted features from 3 different 2D views of each nodule, then input into 2-stage classifier (independent predictions on each view first, then outputs combined into second classifier).



Ciompi et al. Automatic classification of pulmonary peri-fissural nodules in computed tomography using an ensemble of 2D views and a convolutional neural network out-of-the-box. *Medical Image Analysis*, 2015.

Gulshan et al. 2016

- **Task:** Binary classification of referable diabetic retinopathy from **retinal fundus photographs**
- **Input:** Retinal fundus photographs
- **Output:** Binary classification of referable diabetic retinopathy (y in $\{0,1\}$)
 - Defined as moderate and worse diabetic retinopathy, referable diabetic macular edema, or both



Gulshan, et al. Development and Validation of a Deep Learning Algorithm for Detection of Diabetic Retinopathy in Retinal Fundus Photographs. JAMA, 2016.

Gulshan et al. 2016

- **Dataset:**
 - 128,175 images, each graded by 3-7 ophthalmologists.
 - 54 total graders, each paid to grade between 20 to 62508 images.
- **Data preprocessing:**
 - Circular mask of each image was detected and rescaled to be 299 pixels wide
- **Model:**
 - Inception-v3 CNN, with ImageNet pre-training
 - Multiple BCE losses corresponding to different binary prediction problems, which were then used for final determination of referable diabetic retinopathy

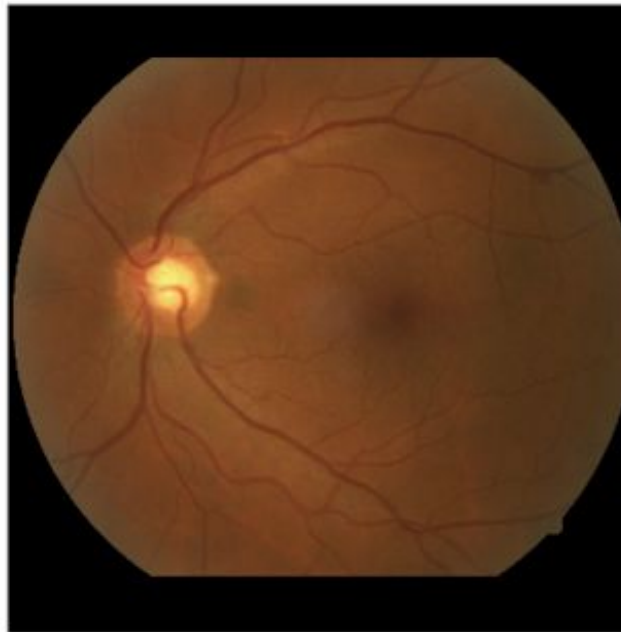


Gulshan, et al. Development and Validation of a Deep Learning Algorithm for Detection of Diabetic Retinopathy in Retinal Fundus Photographs. JAMA, 2016.

Gulshan et al. 2016

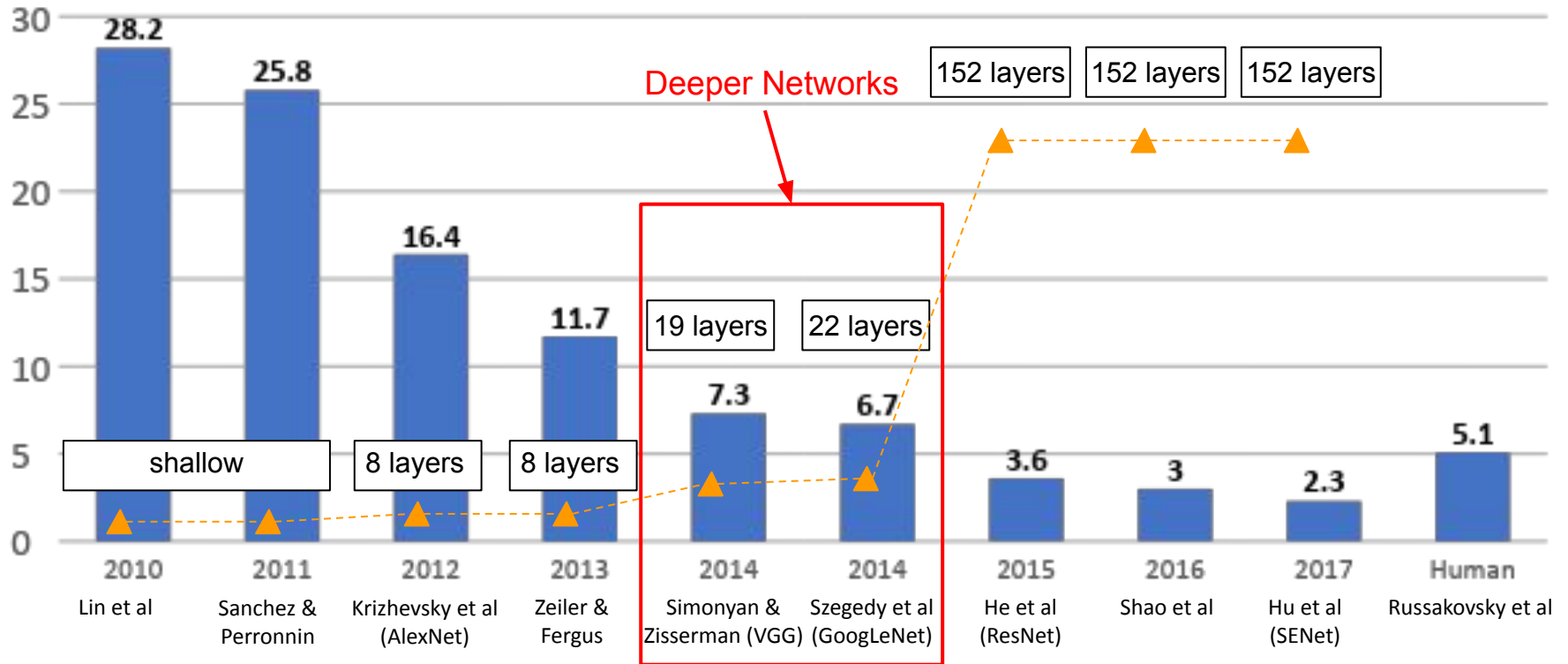
- **Dataset:**
 - 128,175 images, each graded by 3-7 ophthalmologists.
 - 54 total graders, each paid to grade between 20 to 62508 images.
- **Data preprocessing:**
 - Circular mask of each image was detected and rescaled to be 299 pixels wide
- **Model:**
 - Inception-v3 CNN, with ImageNet pre-training
 - Multiple BCE losses corresponding to different binary prediction problems, which were then used for final determination of referable diabetic retinopathy

Graders provided finer-grained labels which were then consolidated into (easier) binary prediction problems



Gulshan, et al. Development and Validation of a Deep Learning Algorithm for Detection of Diabetic Retinopathy in Retinal Fundus Photographs. JAMA, 2016.

ImageNet Large Scale Visual Recognition Challenge (ILSVRC) winners



Slide credit: CS231n

VGGNet

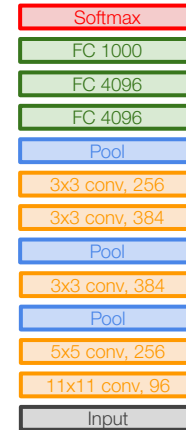
[Simonyan and Zisserman, 2014]

Small filters, Deeper networks

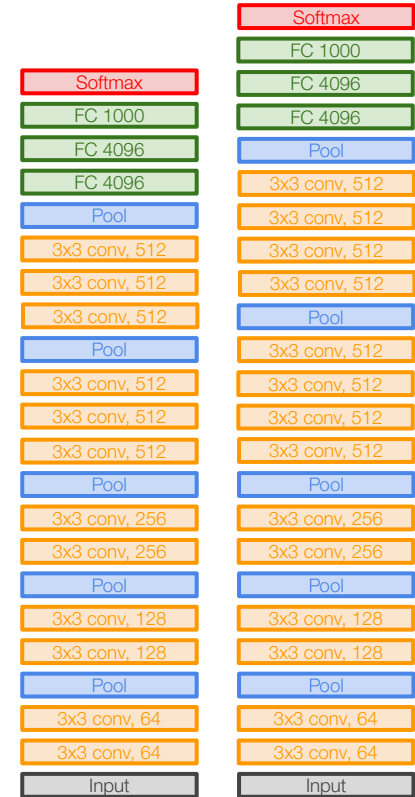
8 layers (AlexNet)

-> 16 - 19 layers (VGG16Net)

Only 3x3 CONV stride 1, pad 1
and 2x2 MAX POOL stride 2



AlexNet



VGG16

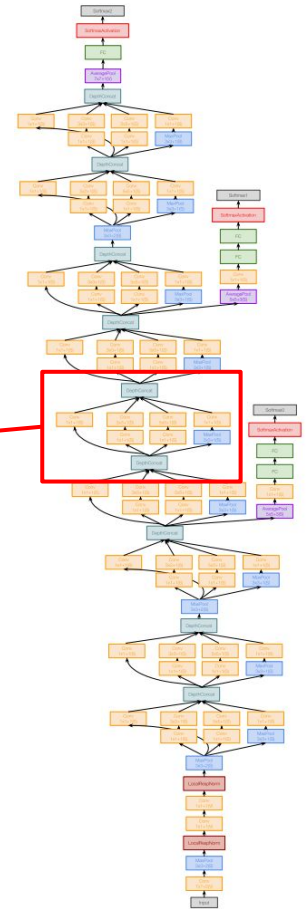
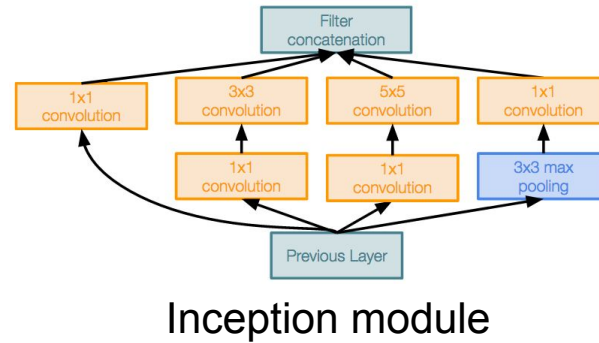
VGG19

Slide credit: CS231n

GoogLeNet

[Szegedy et al., 2014]

“Inception module”: design a good local network topology (network within a network) and then stack these modules on top of each other



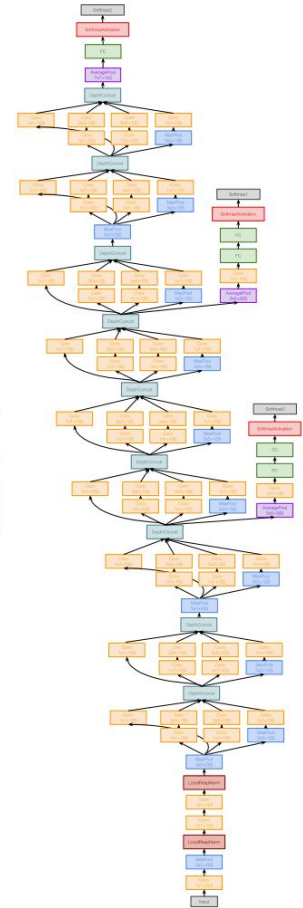
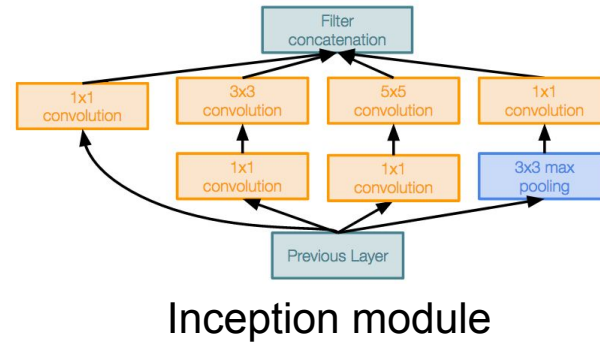
Slide credit: CS231n

GoogLeNet

[Szegedy et al., 2014]

Deeper networks, with computational efficiency

- 22 layers
- Efficient “Inception” module
- Avoids expensive FC layers using a global averaging layer
- 12x less params than AlexNet



Slide credit: CS231n

GoogLeNet

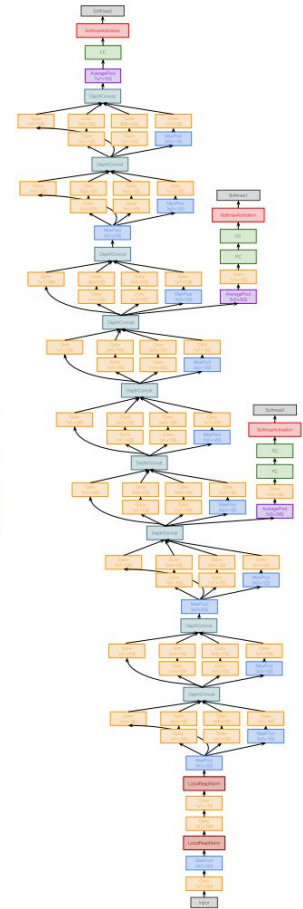
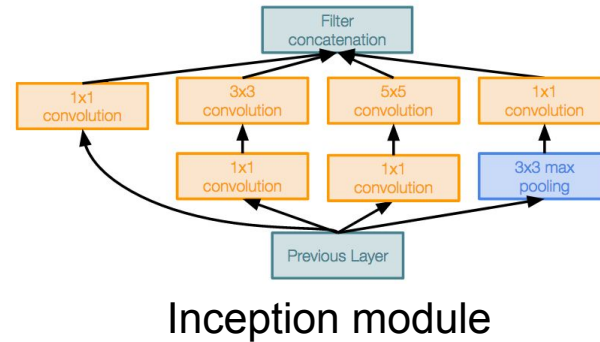
[Szegedy et al., 2014]

Deeper networks, with computational efficiency

- 22 layers
- Efficient “Inception” module
- Avoids expensive FC layers using a global averaging layer
- 12x less params than AlexNet

Also called “Inception Network”

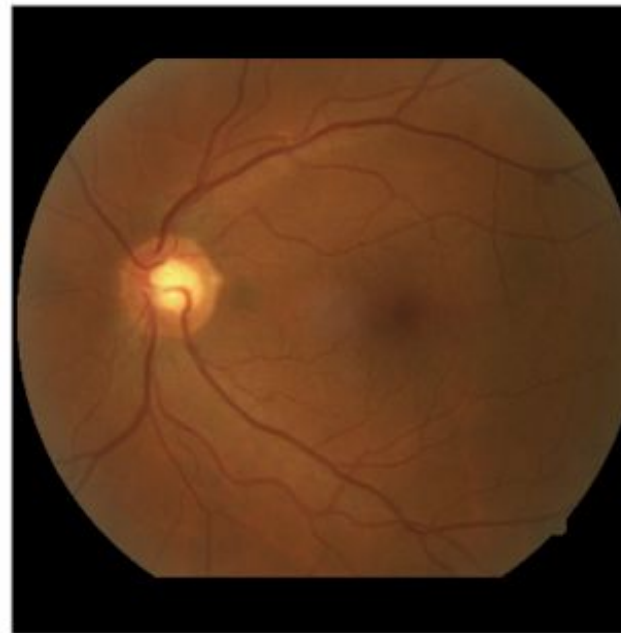
Slide credit: CS231n



Gulshan et al. 2016

- **Dataset:**
 - 128,175 images, each graded by 3-7 ophthalmologists.
 - 54 total graders, each paid to grade between 20 to 62508 images.
- **Data preprocessing:**
 - Circular mask of each image was detected and rescaled to be 299 pixels wide
- **Model:**
 - Inception-v3 CNN, with ImageNet pre-training
 - Multiple BCE losses corresponding to different binary prediction problems, which were then used for final determination of referable diabetic retinopathy

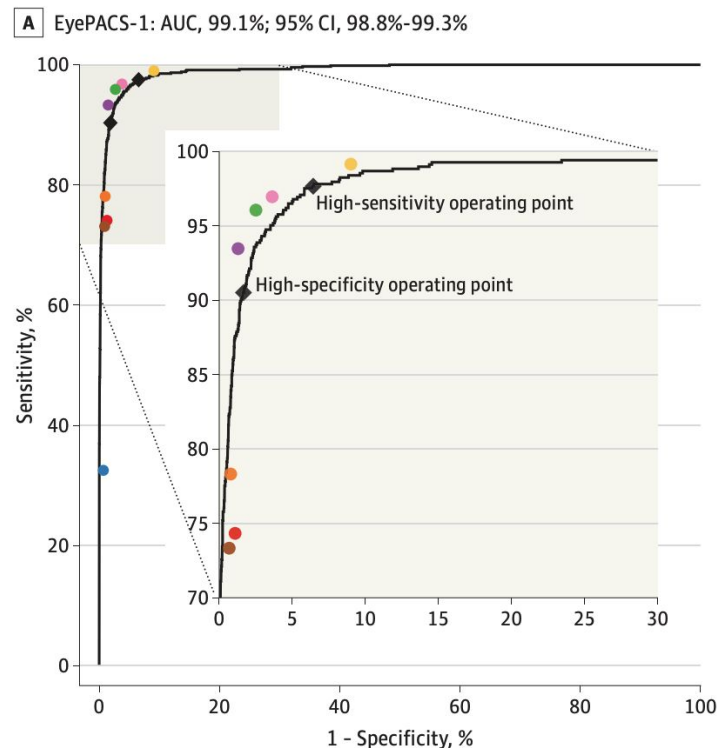
Graders provided finer-grained labels which were then consolidated into (easier) binary prediction problems



Gulshan, et al. Development and Validation of a Deep Learning Algorithm for Detection of Diabetic Retinopathy in Retinal Fundus Photographs. JAMA, 2016.

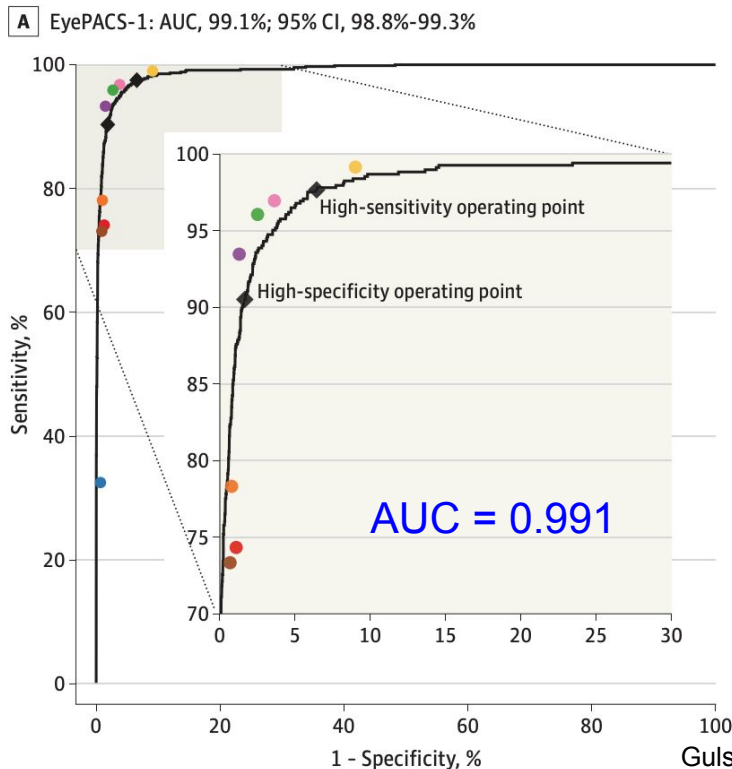
Gulshan et al. 2016

- **Results:**
 - Evaluated using ROC curves, AUC, sensitivity and specificity analysis



Gulshan, et al. Development and Validation of a Deep Learning Algorithm for Detection of Diabetic Retinopathy in Retinal Fundus Photographs. JAMA, 2016.

Gulshan et al. 2016



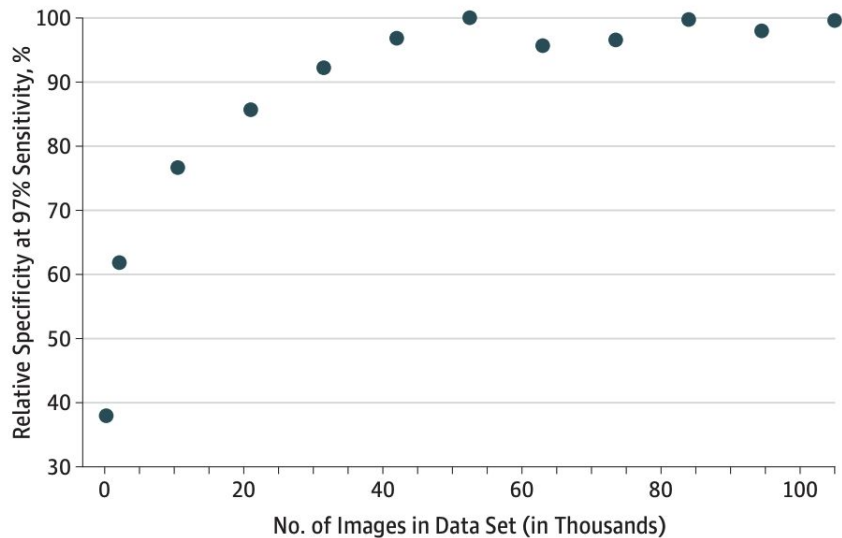
Looked at different operating points

- High-specificity point approximated ophthalmologist specificity for comparison. Should also use high-specificity to make decisions about high-risk actions.
- High-sensitivity point should be used for screening applications.

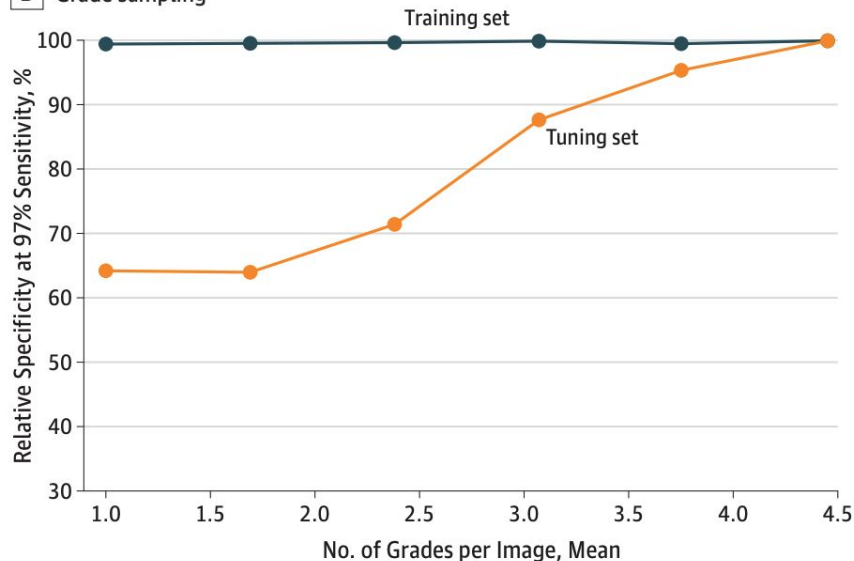
Gulshan, et al. Development and Validation of a Deep Learning Algorithm for Detection of Diabetic Retinopathy in Retinal Fundus Photographs. JAMA, 2016.

Gulshan et al. 2016

A Image sampling



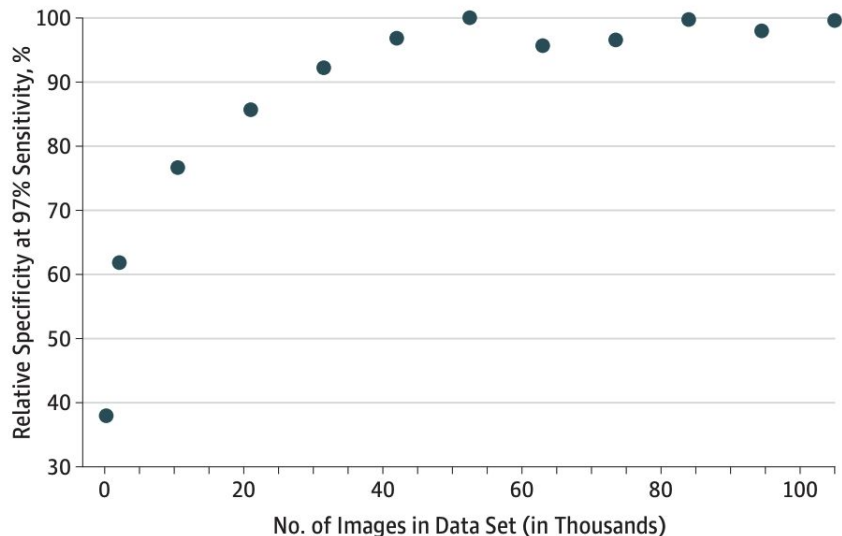
B Grade sampling



Gulshan, et al. Development and Validation of a Deep Learning Algorithm for Detection of Diabetic Retinopathy in Retinal Fundus Photographs. JAMA, 2016.

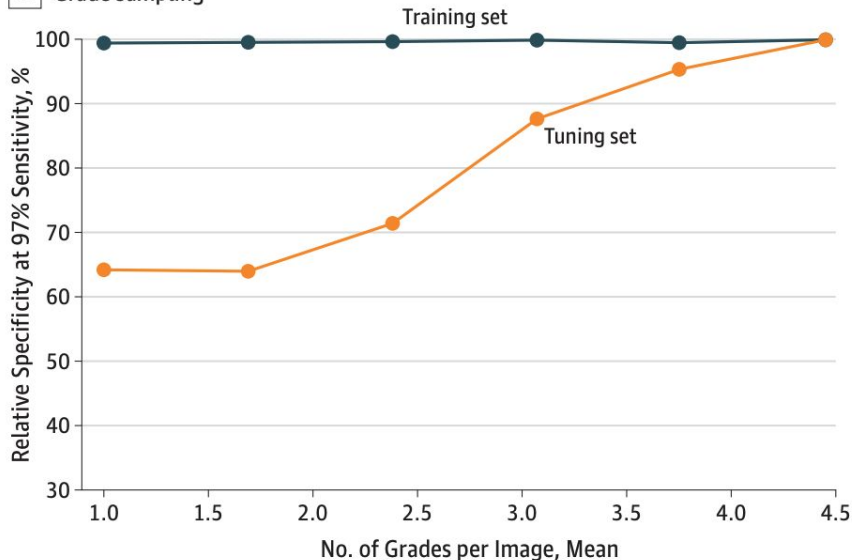
Gulshan et al. 2016

A Image sampling



Q: What could explain the difference in trends for reducing # grades / image on training set vs. tuning set, on tuning set performance?

B Grade sampling



Gulshan, et al. Development and Validation of a Deep Learning Algorithm for Detection of Diabetic Retinopathy in Retinal Fundus Photographs. JAMA, 2016.

Considering multiple possible sources of data

E.g., some with noisier / less accurate labels than others, from different hospital sites, etc.

- Expected diversity of data during deployment should be reflected in both training and test sets
 - Need to see these during training to learn how to handle them
 - Need to see these during testing to accurately evaluate the model

Considering multiple possible sources of data

E.g., some with noisier / less accurate labels than others, from different hospital sites, etc.

- Expected diversity of data during deployment should be reflected in both training and test sets
 - Need to see these during training to learn how to handle them
 - Need to see these during testing to accurately evaluate the model
- Want test set labels to be as accurate as possible

Considering multiple possible sources of data

E.g., some with noisier / less accurate labels than others, from different hospital sites, etc.

- Expected diversity of data during deployment should be reflected in both training and test sets
 - Need to see these during training to learn how to handle them
 - Need to see these during testing to accurately evaluate the model
- Want test set labels to be as accurate as possible
- Noisy labels is often still useful during training -- can provide useful signal in aggregate. Much larger amount, but noisy, data is *sometimes* better than small but clean data.
 - “Weakly supervised learning” is a major area of research focused on learning with large amounts of noisy or imprecise labels

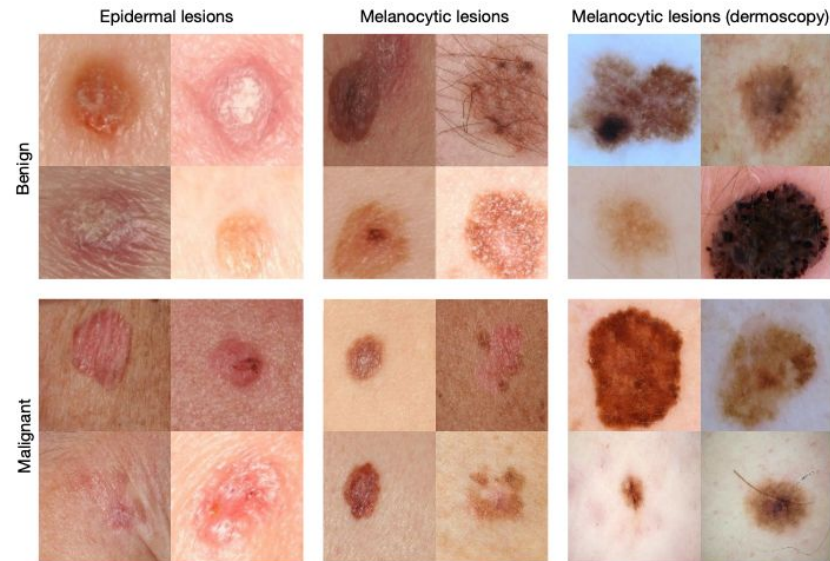
Preview: advanced approaches for handling limited labeled data

- Semi-supervised learning
- Self-supervised learning
- Weakly supervised learning

Will talk more about these in later lectures...

Esteva et al. 2017

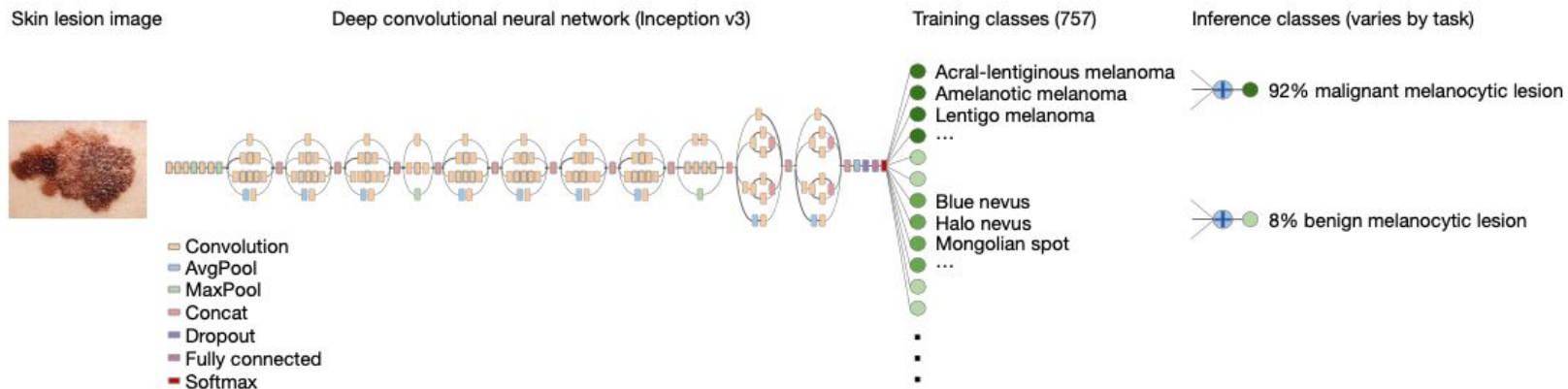
- Two binary classification tasks: malignant vs. benign lesions of epidermal or melanocytic origin
- Inception-v3 (GoogLeNet) CNN with ImageNet pre-training
- Fine-tuned on dataset of 129,450 lesions (from several sources) comprising 2,032 diseases
- Evaluated model vs. 21 or more dermatologists in various settings



Esteva*, Kuprel*, et al. Dermatologist-level classification of skin cancer with deep neural networks. Nature, 2017.

Esteva et al. 2017

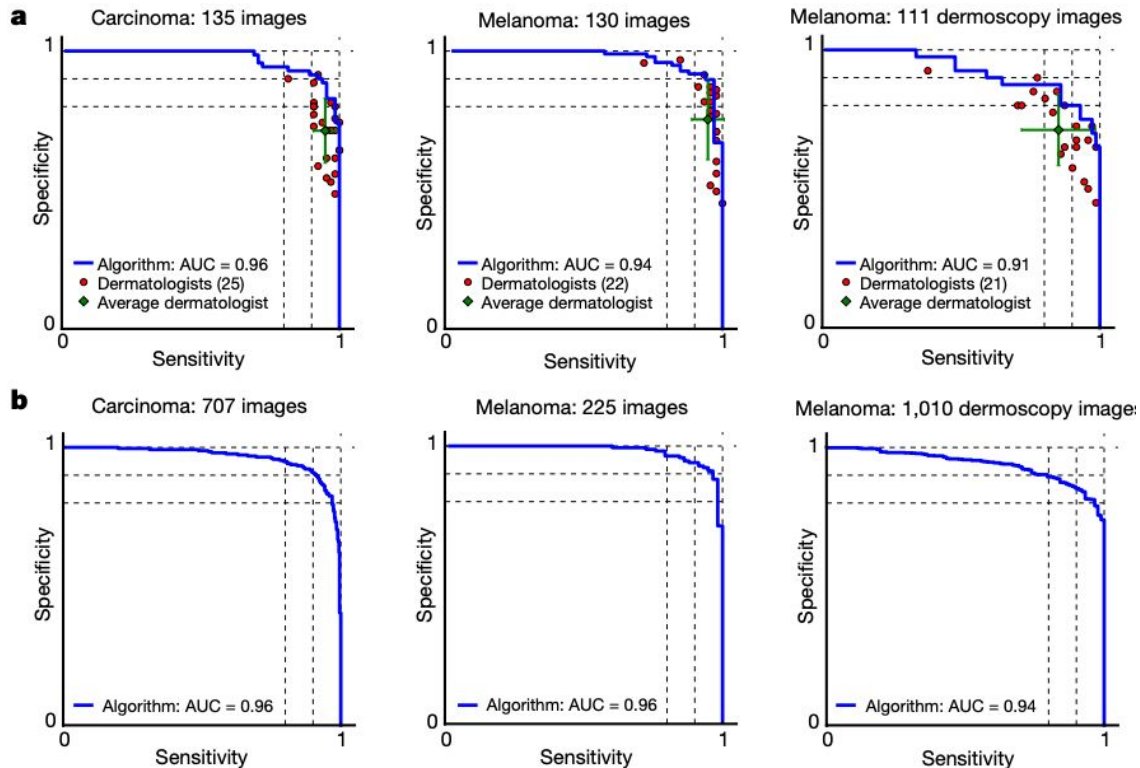
- Train on finer-grained classification (757 classes) but perform binary classification at inference time by summing probabilities of fine-grained sub-classes
- The stronger fine-grained supervision during the training stage improves inference performance!



Esteva*, Kuprel*, et al. Dermatologist-level classification of skin cancer with deep neural networks. Nature, 2017.

Esteva et al. 2017

- Evaluation of algorithm vs. dermatologists



Esteva*, Kuprel*, et al. Dermatologist-level classification of skin cancer with deep neural networks. Nature, 2017.

Lakhani and Sundaram 2017

- Binary classification of pulmonary tuberculosis from x-rays
- Four de-identified datasets
- 1007 chest x-rays (68% train, 17.1% validation, 14.9% test)
- Tried training CNNs from scratch as well as fine-tuning from ImageNet

AUC Test Dataset

Parameter	Untrained	Pretrained	Untrained with Augmentation*	Pretrained with Augmentation*
AlexNet	0.90 (0.84, 0.95)	0.98 (0.95, 1.00)	0.95 (0.90, 0.98)	0.98 (0.94, 0.99)
GoogLeNet	0.88 (0.81, 0.92)	0.97 (0.93, 0.99)	0.94 (0.89, 0.97)	0.98 (0.94, 1.00)
Ensemble				0.99 (0.96, 1.00)

Note.—Data in parentheses are 95% confidence interval.

* Additional augmentation of 90, 180, 270 rotations, and Contrast Limited Adaptive Histogram Equalization processing.

Lakhani and Sundaram 2017

- Binary classification of pulmonary tuberculosis from x-rays
- Four de-identified datasets
- 1007 chest x-rays (68% train, 17.1% validation, 14.9% test)
- Tried training CNNs from scratch as well as fine-tuning from ImageNet

AUC Test Dataset

Parameter	Untrained	Pretrained	Untrained with Augmentation*	Pretrained with Augmentation*
AlexNet	0.90 (0.84, 0.95)	0.98 (0.95, 1.00)	0.95 (0.90, 0.98)	0.98 (0.94, 0.99)
GoogLeNet	0.88 (0.81, 0.92)	0.97 (0.93, 0.99)	0.94 (0.89, 0.97)	0.98 (0.94, 1.00)
Ensemble				0.99 (0.96, 1.00)

Note.—Data in parentheses are 95% confidence interval.

* Additional augmentation of 90, 180, 270 rotations, and Contrast Limited Adaptive Histogram Equalization processing.

All training images were resized to 256x256 and underwent base data augmentation of random 227x227 cropping and mirror images. Additional data augmentation experiments in results table.

Lakhani and Sundaram. Deep learning at chest radiography: Automated Classification of Pulmonary Tuberculosis by Using Convolutional Neural Networks. Radiology, 2017.

Lakhani and Sundaram 2017

- Binary classification of pulmonary tuberculosis from x-rays
- Four de-identified datasets
- 1007 chest x-rays (68% train, 17.1% validation, 14.9% test)
- Tried training CNNs from scratch as well as fine-tuning from ImageNet

AUC Test Dataset

Parameter	Untrained	Pretrained	Untrained with Augmentation*	Pretrained with Augmentation*
AlexNet	0.90 (0.84, 0.95)	0.98 (0.95, 1.00)	0.95 (0.90, 0.98)	0.98 (0.94, 0.99)
GoogLeNet	0.88 (0.81, 0.92)	0.97 (0.93, 0.99)	0.94 (0.89, 0.97)	0.98 (0.94, 1.00)
Ensemble				0.99 (0.96, 1.00)

Note.—Data in parentheses are 95% confidence interval.

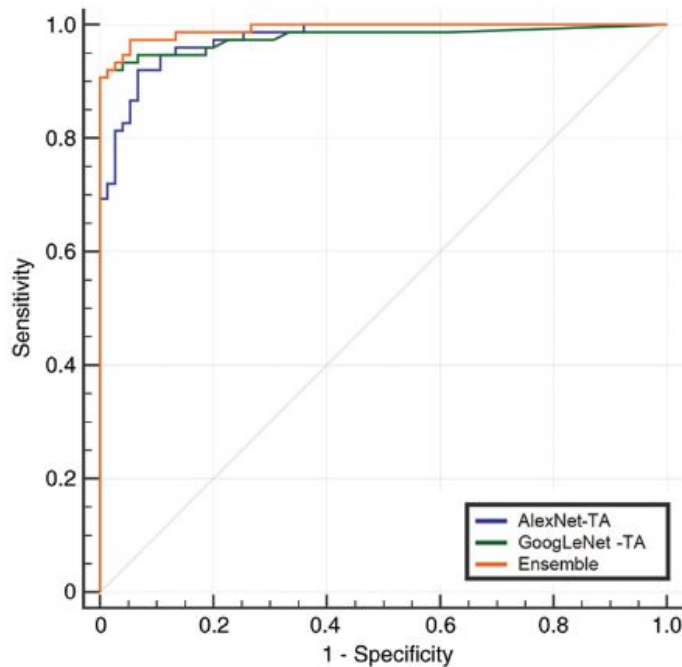
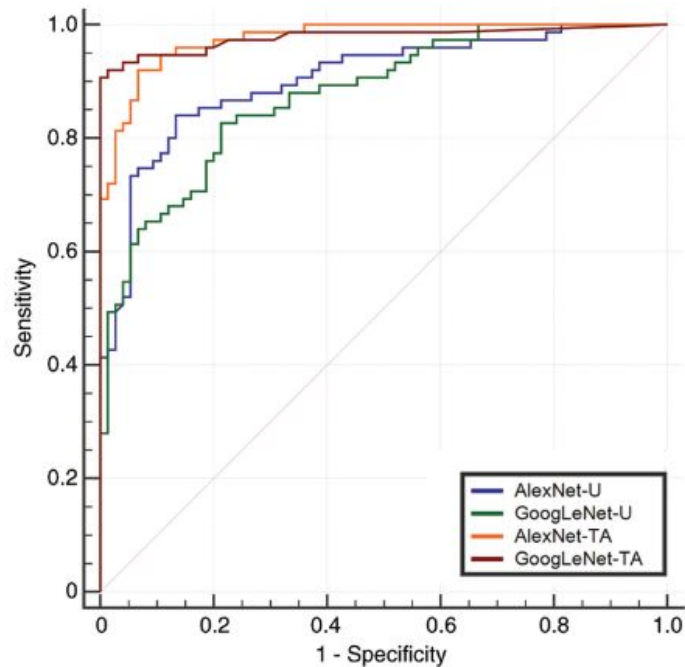
* Additional augmentation of 90, 180, 270 rotations, and Contrast Limited Adaptive Histogram Equalization processing.

All training images were resized to 256x256 and underwent base data augmentation of random 227x227 cropping and mirror images. Additional data augmentation experiments in results table.

Often resize to match input size of pre-trained networks. Also fine approach to making high-res dataset easier to work with!

Lakhani and Sundaram. Deep learning at chest radiography: Automated Classification of Pulmonary Tuberculosis by Using Convolutional Neural Networks. Radiology, 2017.

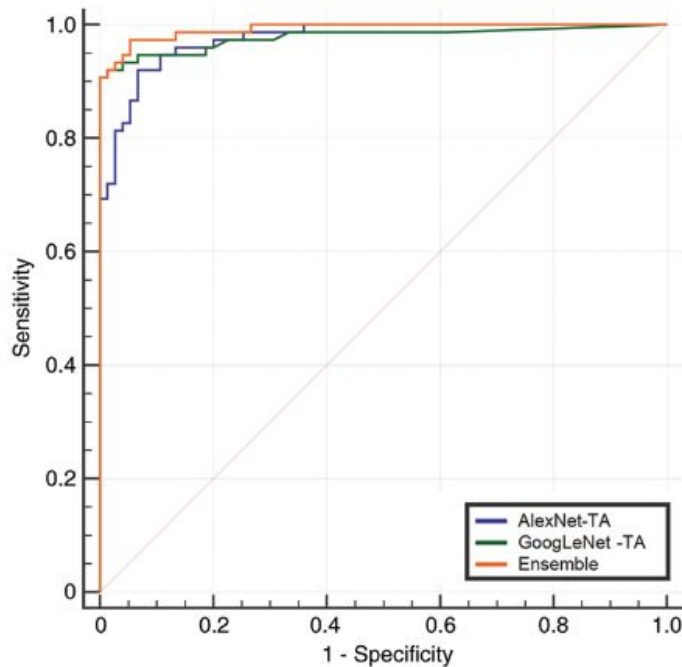
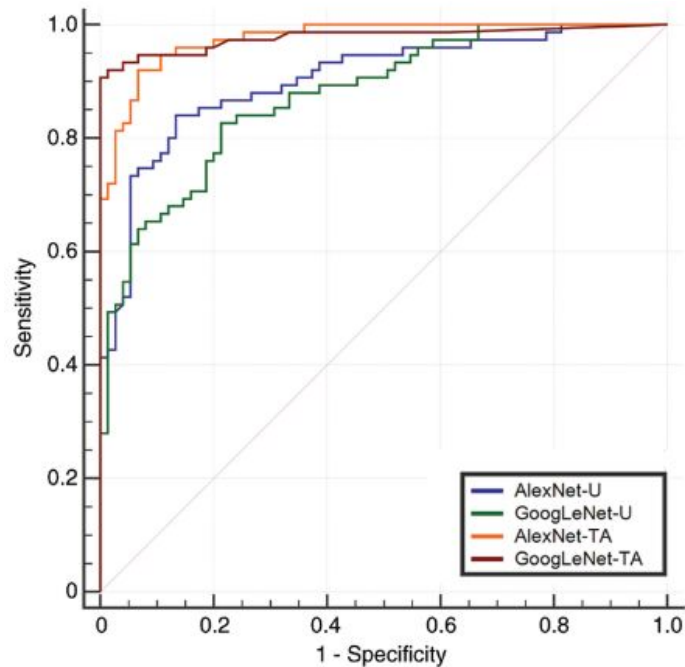
Lakhani and Sundaram 2017



Lakhani and Sundaram. Deep learning at chest radiography: Automated Classification of Pulmonary Tuberculosis by Using Convolutional Neural Networks. Radiology, 2017.

Lakhani and Sundaram 2017

Performed further analysis at optimal threshold determined by the Youden Index.



Lakhani and Sundaram. Deep learning at chest radiography: Automated Classification of Pulmonary Tuberculosis by Using Convolutional Neural Networks. Radiology, 2017.

Rajpurkar et al. 2017

- Binary classification of pneumonia presence in chest X-rays
- Used ChestX-ray14 dataset with over 100,000 frontal X-ray images with 14 diseases
- 121-layer DenseNet CNN
- Compared algorithm performance with 4 radiologists
- Also applied algorithm to other diseases to surpass previous state-of-the-art on ChestX-ray14



Input

Chest X-Ray Image

CheXNet

121-layer CNN

Output

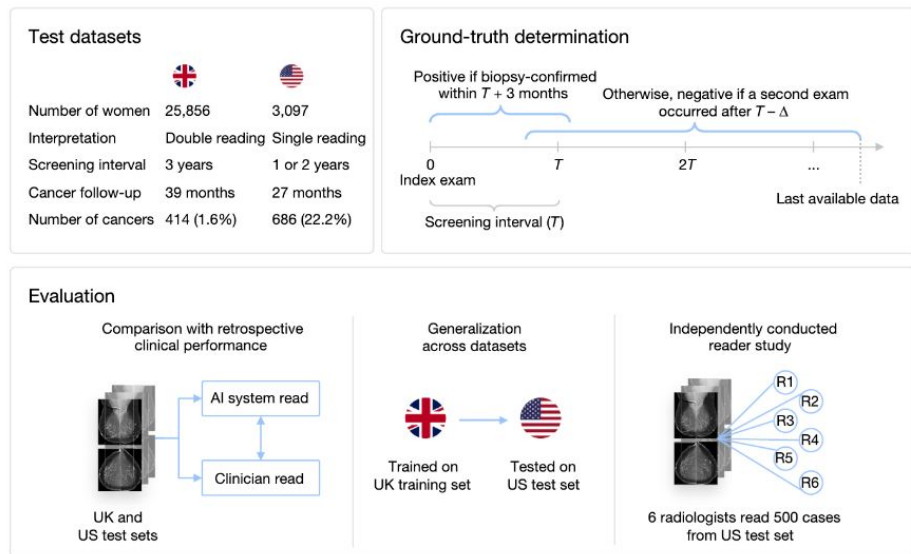
Pneumonia Positive (85%)



Rajpurkar et al. CheXNet: Radiologist-Level Pneumonia Detection on Chest X-Rays with Deep Learning. 2017.

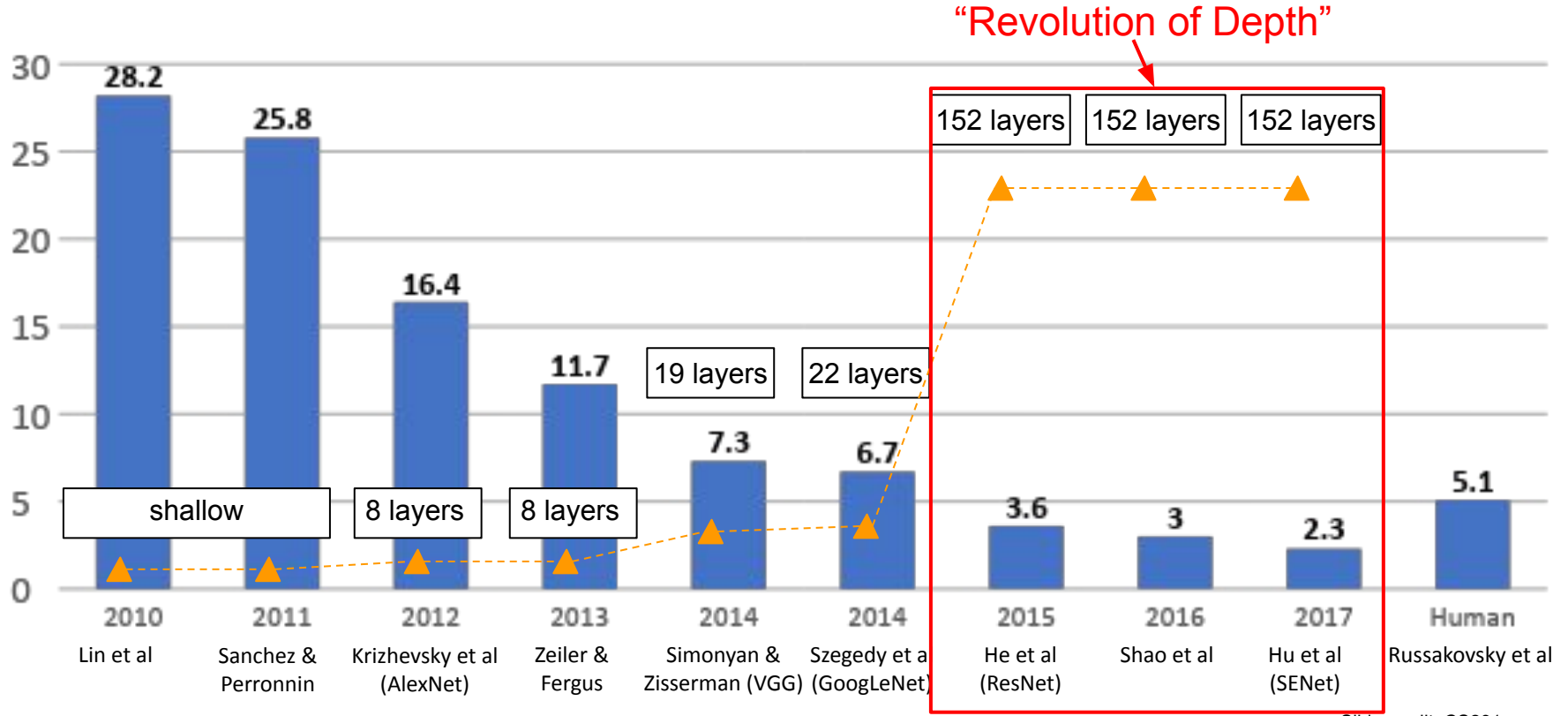
McKinney et al. 2020

- Binary classification of breast cancer in mammograms
- Used an ensemble of models including ResNets
- International dataset and evaluation, across UK and US



McKinney et al. International evaluation of an AI system for breast cancer screening. Nature, 2020.

ImageNet Large Scale Visual Recognition Challenge (ILSVRC) winners



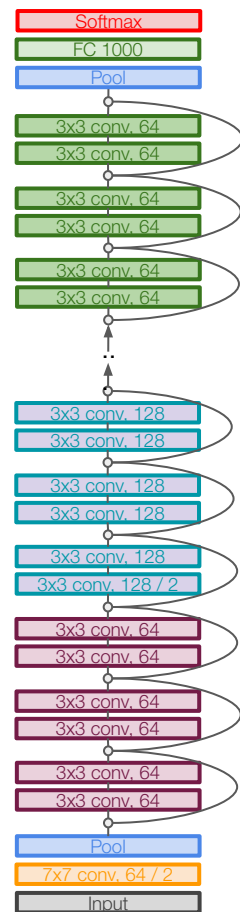
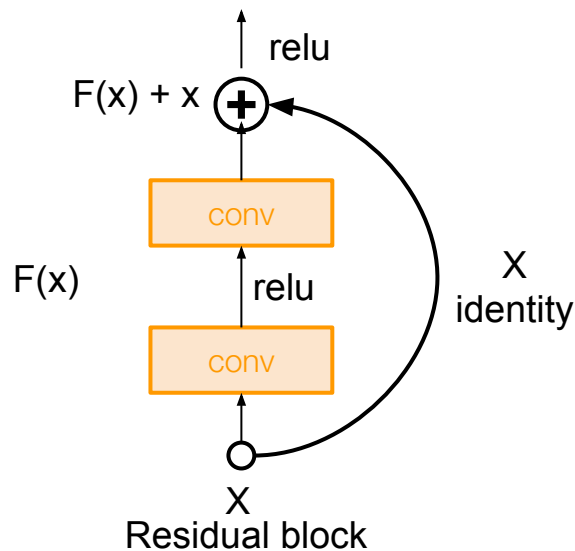
Slide credit: CS231n

ResNet

[He et al., 2015]

Very deep networks using residual connections

- 152-layer model for ImageNet
- Won all major classification and detection benchmark challenges in 2015

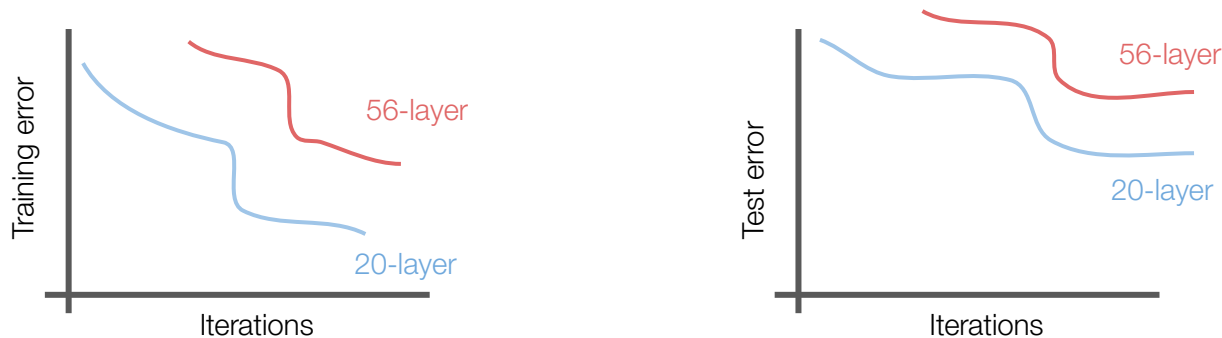


Slide credit: CS231n

ResNet

[He et al., 2015]

What happens when we continue stacking deeper layers on a “plain” convolutional neural network?



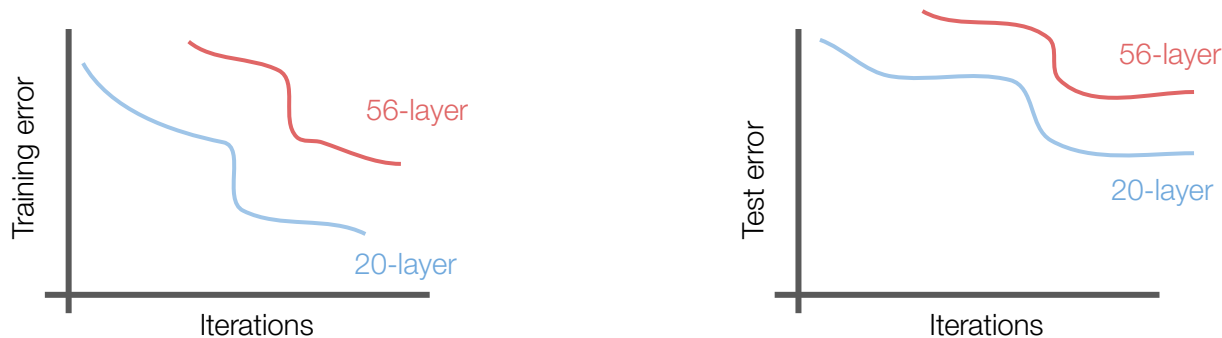
Q: What's strange about these training and test curves?
[Hint: look at the order of the curves]

Slide credit: CS231n

ResNet

[He et al., 2015]

What happens when we continue stacking deeper layers on a “plain” convolutional neural network?



56-layer model performs worse on both training and test error
-> The deeper model performs worse, but it's not caused by overfitting!

Slide credit: CS231n

ResNet

[He et al., 2015]

Hypothesis: the problem is an *optimization* problem, deeper models are harder to optimize

Slide credit: CS231n

ResNet

[He et al., 2015]

Hypothesis: the problem is an *optimization* problem, deeper models are harder to optimize

The deeper model should be able to perform at least as well as the shallower model.

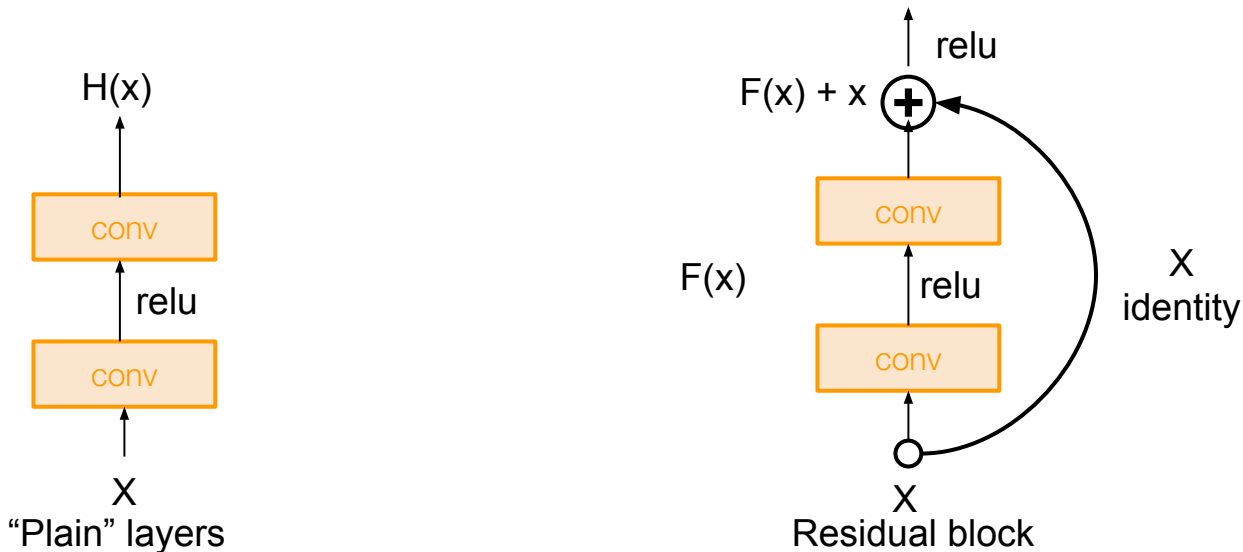
A solution by construction is copying the learned layers over from the shallower model and setting all additional layers to the **identity** function.

Slide credit: CS231n

ResNet

[He et al., 2015]

Solution: Structure each network layer to fit a “residual function” with respect to the identity function, then add the two functions together



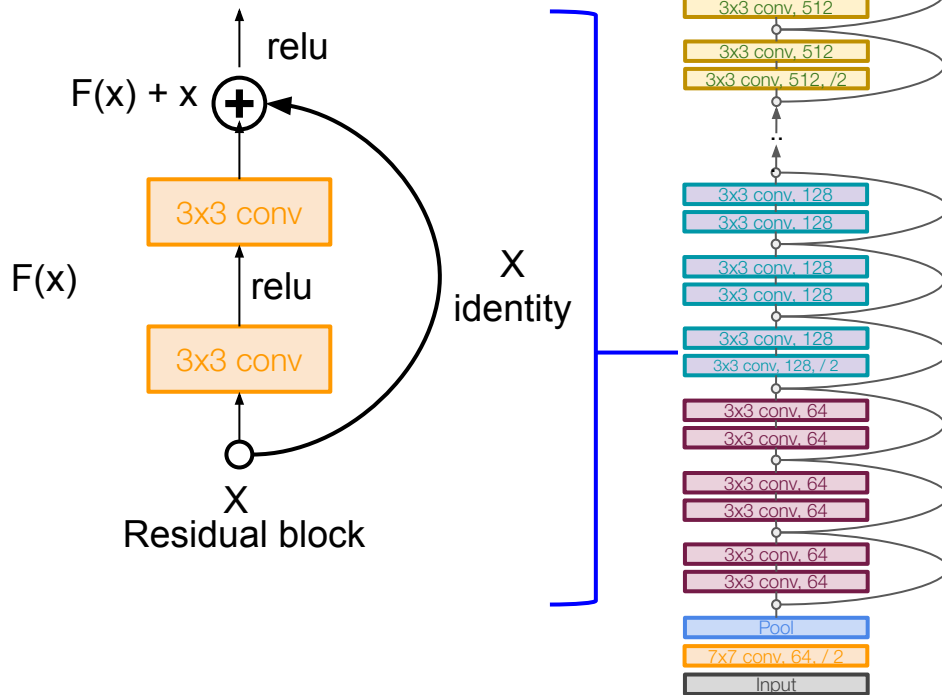
Slide credit: CS231n

ResNet

[He et al., 2015]

Full ResNet architecture:

- Stack residual blocks
- Every residual block has two 3x3 conv layers



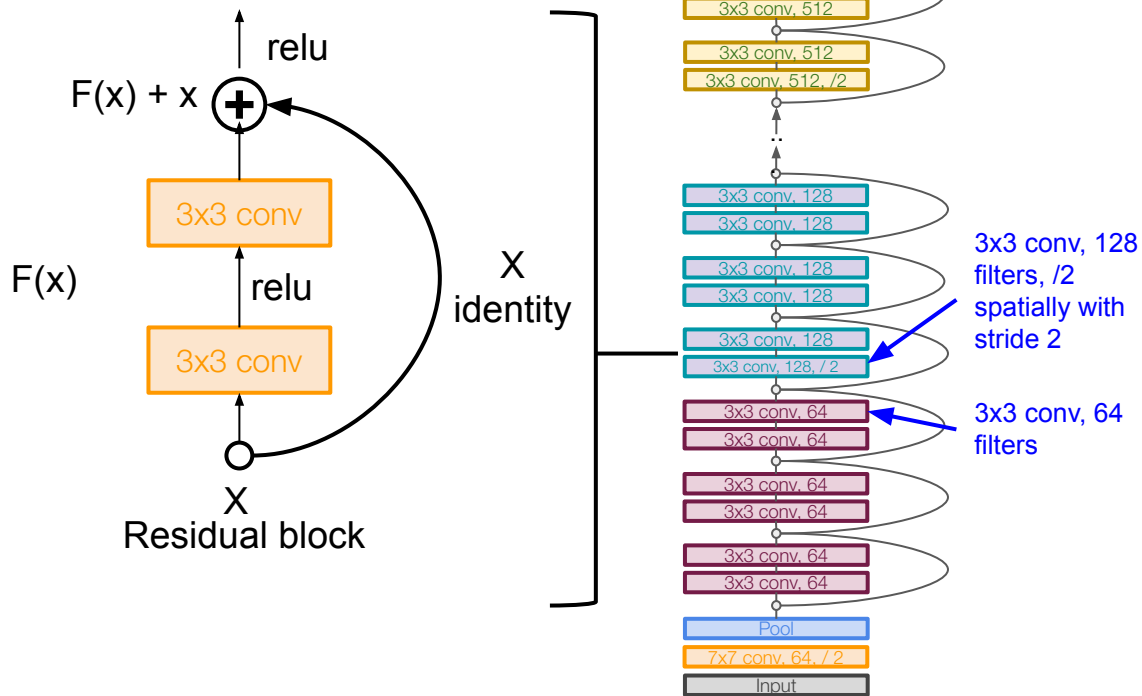
Slide credit: CS231n

ResNet

[He et al., 2015]

Full ResNet architecture:

- Stack residual blocks
- Every residual block has two 3x3 conv layers
- Periodically, double # of filters and downsample spatially using stride 2 (/2 in each dimension)



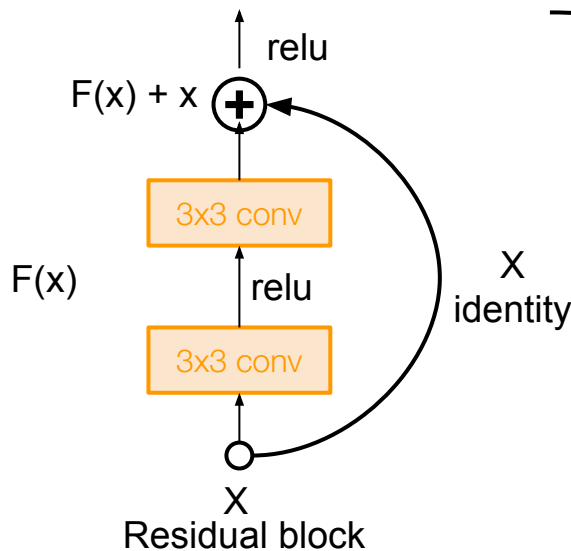
Slide credit: CS231n

ResNet

[He et al., 2015]

Full ResNet architecture:

- Stack residual blocks
- Every residual block has two 3x3 conv layers
- Periodically, double # of filters and downsample spatially using stride 2 (/2 in each dimension)
- Additional conv layer at the beginning



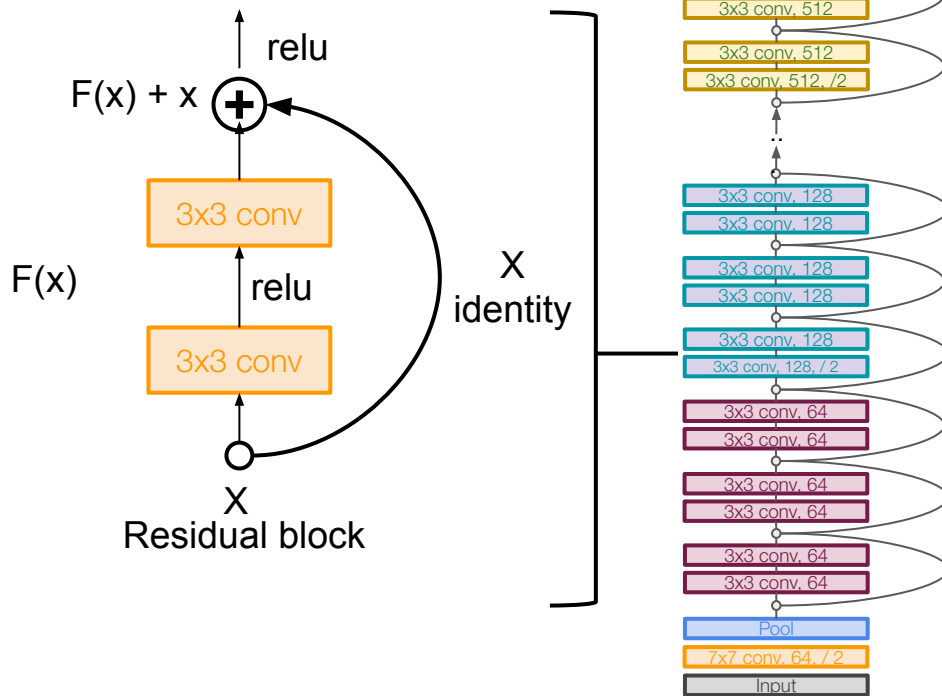
Slide credit: CS231n

ResNet

[He et al., 2015]

Full ResNet architecture:

- Stack residual blocks
- Every residual block has two 3x3 conv layers
- Periodically, double # of filters and downsample spatially using stride 2 (/2 in each dimension)
- Additional conv layer at the beginning
- No FC layers at the end (only FC 1000 to output classes)

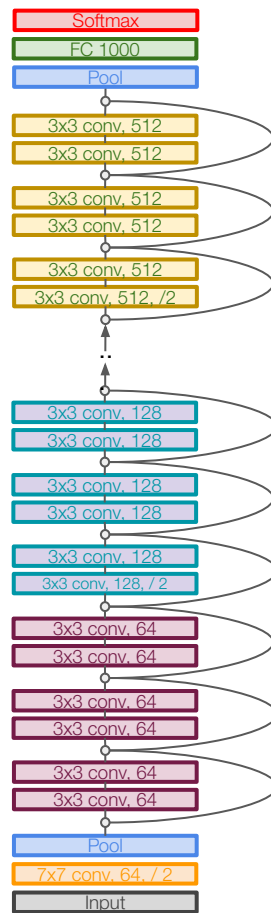


Slide credit: CS231n

ResNet

[He et al., 2015]

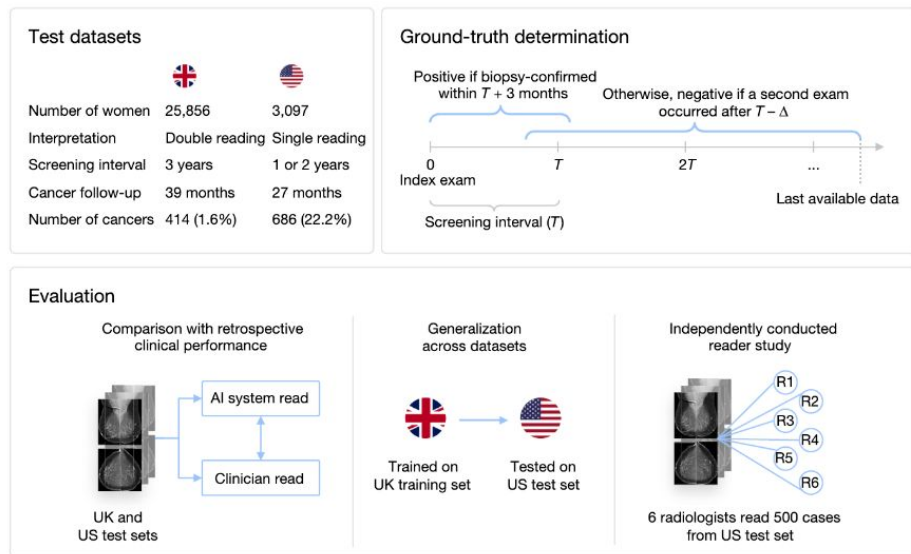
Total depths of 34, 50, 101, or 152 layers for ImageNet



Slide credit: CS231n

McKinney et al. 2020

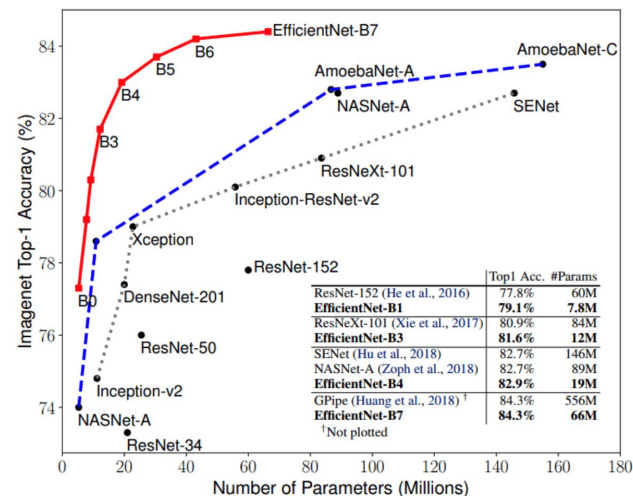
- Binary classification of breast cancer in mammograms
- Used an ensemble of models including ResNets
- International dataset and evaluation, across UK and US



McKinney et al. International evaluation of an AI system for breast cancer screening. Nature, 2020.

More recent CNN architectures

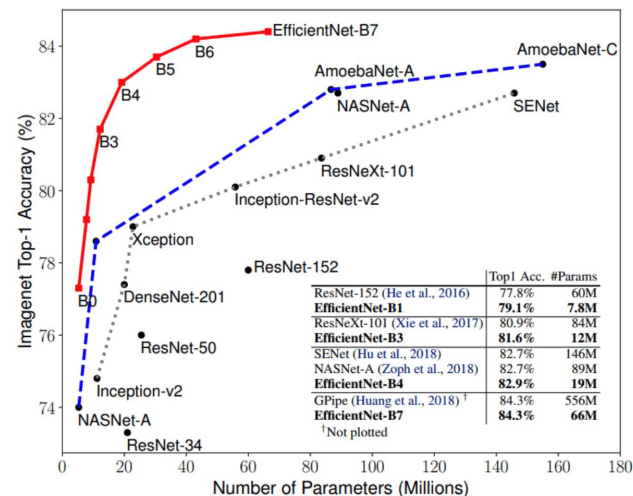
- MobileNet (Sandler et al. 2018) - architecture with separable convolutions for light-weight CNNs
- NASNet (Zoph et al. 2016) and AmoebaNet (Real et al. 2019) - architectures discovered through “neural architecture search” via reinforcement learning or evolutionary algorithms
- EfficientNet (Tan et al. 2020) - family of architectures designed using “compound scaling” that simultaneously scale width, depth, and resolution of neural networks with a fixed ratio



More recent CNN architectures

Worth exploring for class projects!

- MobileNet (Sandler et al. 2018) - architecture with separable convolutions for light-weight CNNs
- NASNet (Zoph et al. 2016) and AmoebaNet (Real et al. 2019) - architectures discovered through “neural architecture search” via reinforcement learning or evolutionary algorithms
- EfficientNet (Tan et al. 2020) - family of architectures designed using “compound scaling” that simultaneously scale width, depth, and resolution of neural networks with a fixed ratio

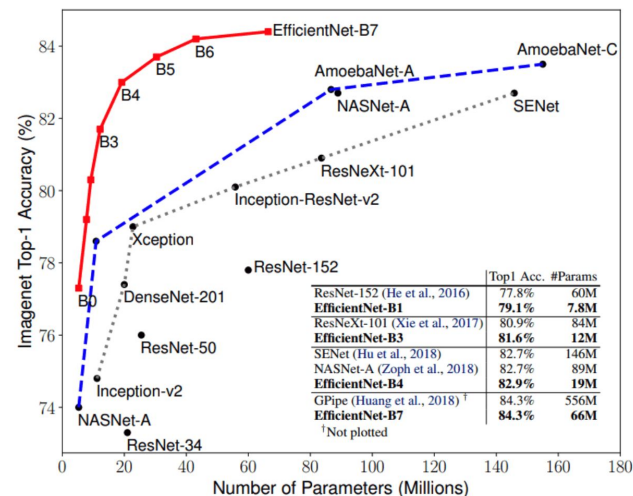


More recent CNN architectures

Worth exploring for class projects!

- MobileNet (Sandler et al. 2018) - architecture with separable convolutions for light-weight CNNs
- NASNet (Zoph et al. 2016) and AmoebaNet (Real et al. 2019) - architectures discovered through “neural architecture search” via reinforcement learning or evolutionary algorithms
- EfficientNet (Tan et al. 2020) - family of architectures designed using “compound scaling” that simultaneously scale width, depth, and resolution of neural networks with a fixed ratio

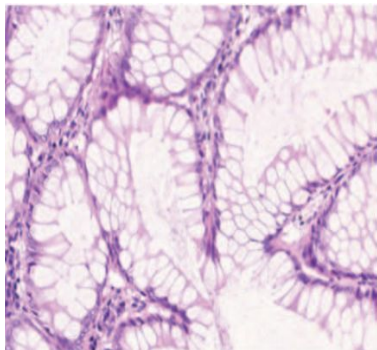
Preview: Transformers, a new class of deep learning architecture, was originally designed for NLP/sequence data but has recently also been applied for computer vision tasks. Stay tuned!



Advanced Vision Models: Segmentation and Detection

Richer visual recognition tasks: segmentation and detection

Classification



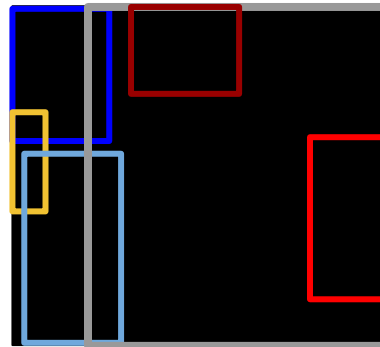
Output:
one category label for
image (e.g., colorectal
glands)

Semantic Segmentation



Output:
category label for each pixel
in the image

Detection



Output:
Spatial bounding box for
each **instance** of a
category object in the
image

Instance Segmentation

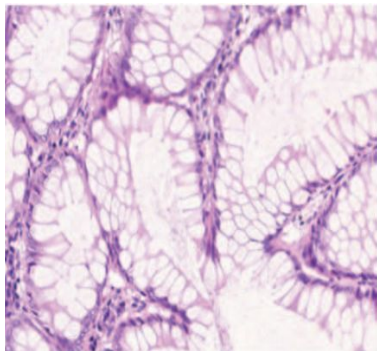


Output:
Category label and instance
label for each pixel in the
image

Figures: Chen et al. 2016. <https://arxiv.org/pdf/1604.02677.pdf>

Richer visual recognition tasks: segmentation and detection

Classification



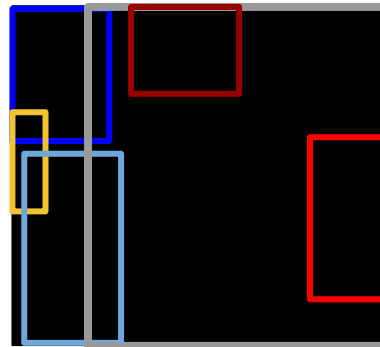
Output:
one category label for
image (e.g., colorectal
glands)

Semantic Segmentation



Output:
category label for each pixel
in the image

Detection



Output:
Spatial bounding box for
each **instance** of a
category object in the
image

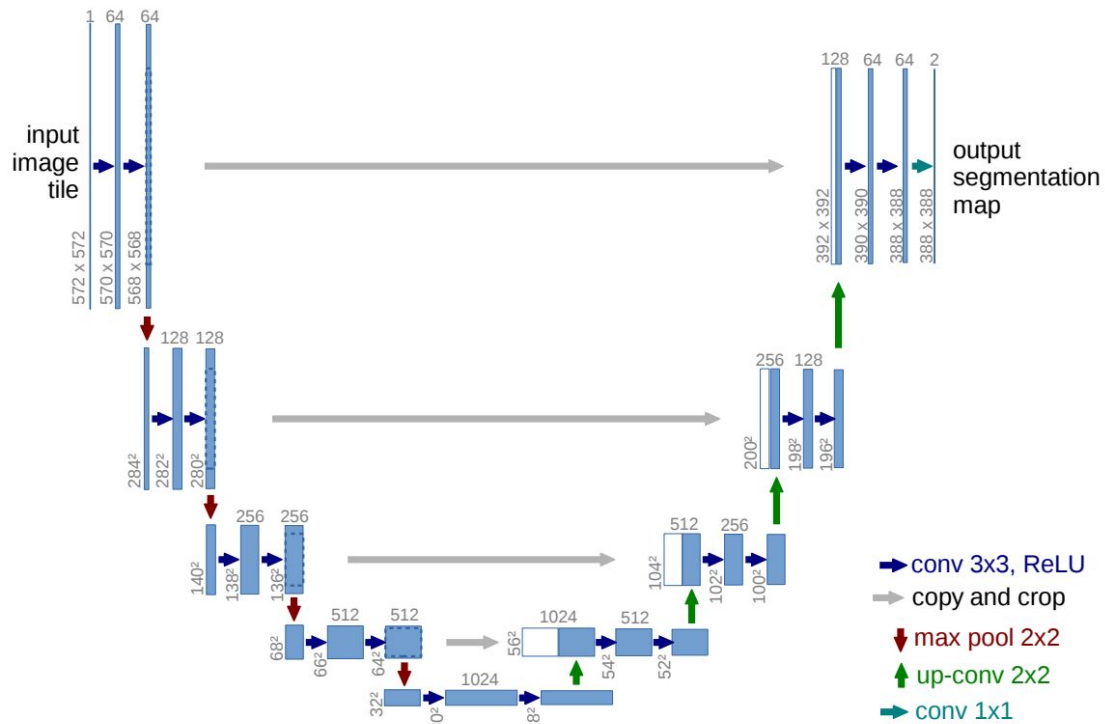
Instance Segmentation



Output:
Category label and instance
label for each pixel in the
image

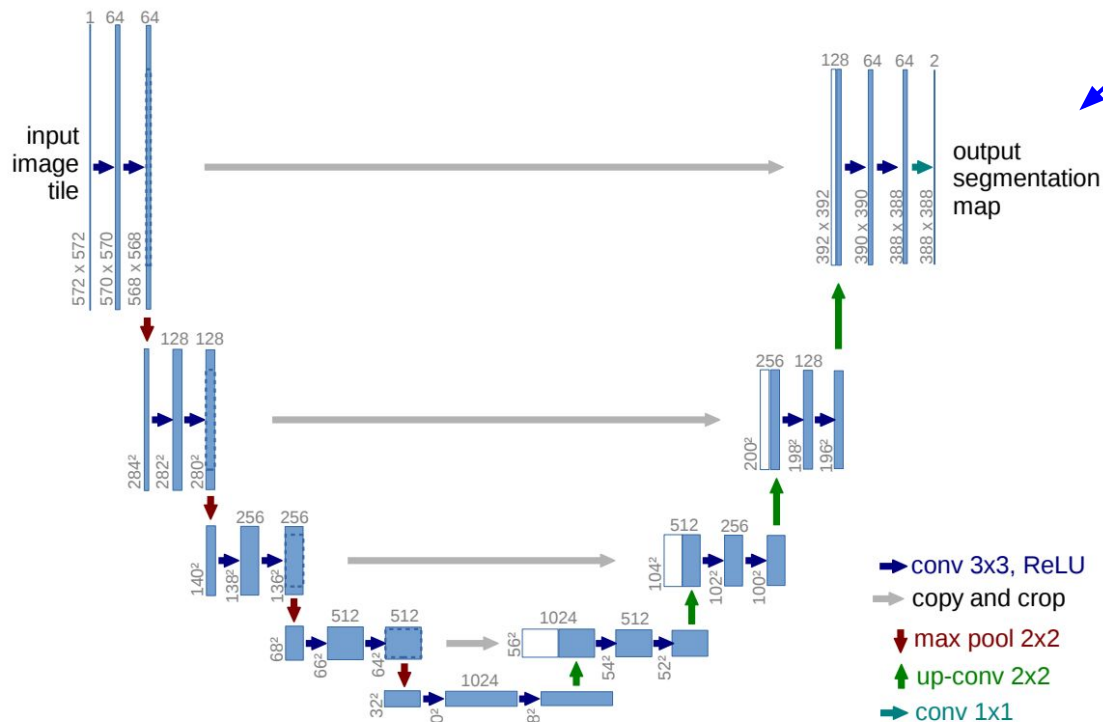
Distinguishes between different instances of an object

Semantic segmentation: U-Net



Ronneberger et al. 2015. U-Net: Convolutional Networks for Biomedical Image Segmentation. 2015.

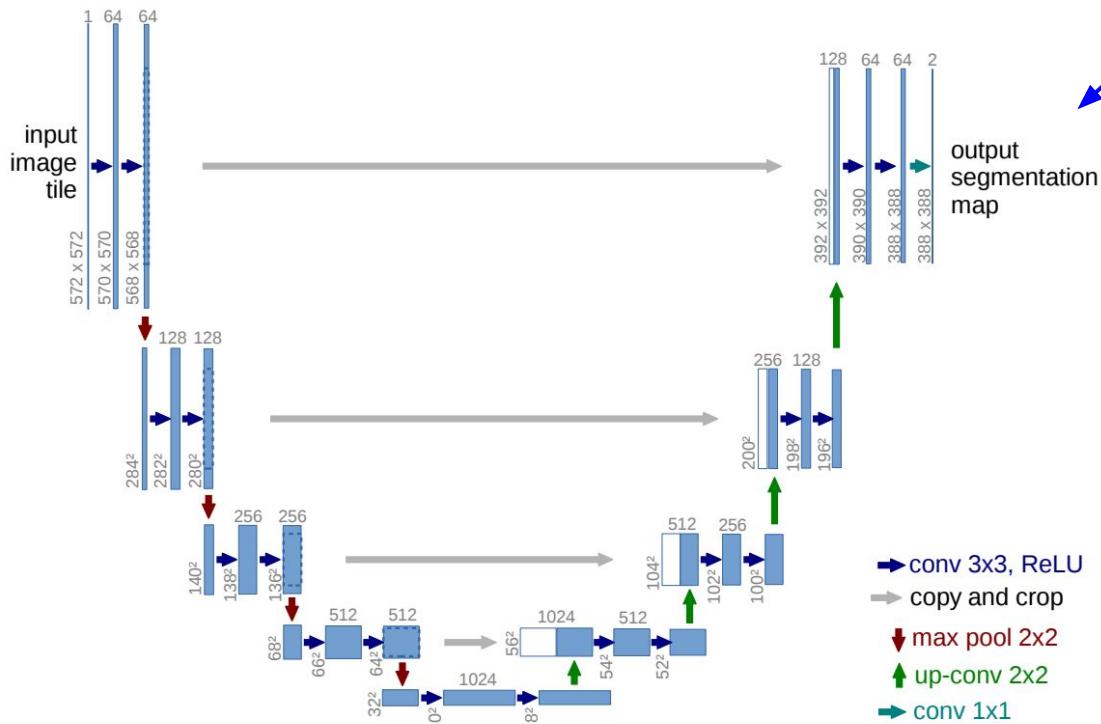
Semantic segmentation: U-Net



Output is an image mask: width x height x # classes

Ronneberger et al. 2015. U-Net: Convolutional Networks for Biomedical Image Segmentation. 2015.

Semantic segmentation: U-Net



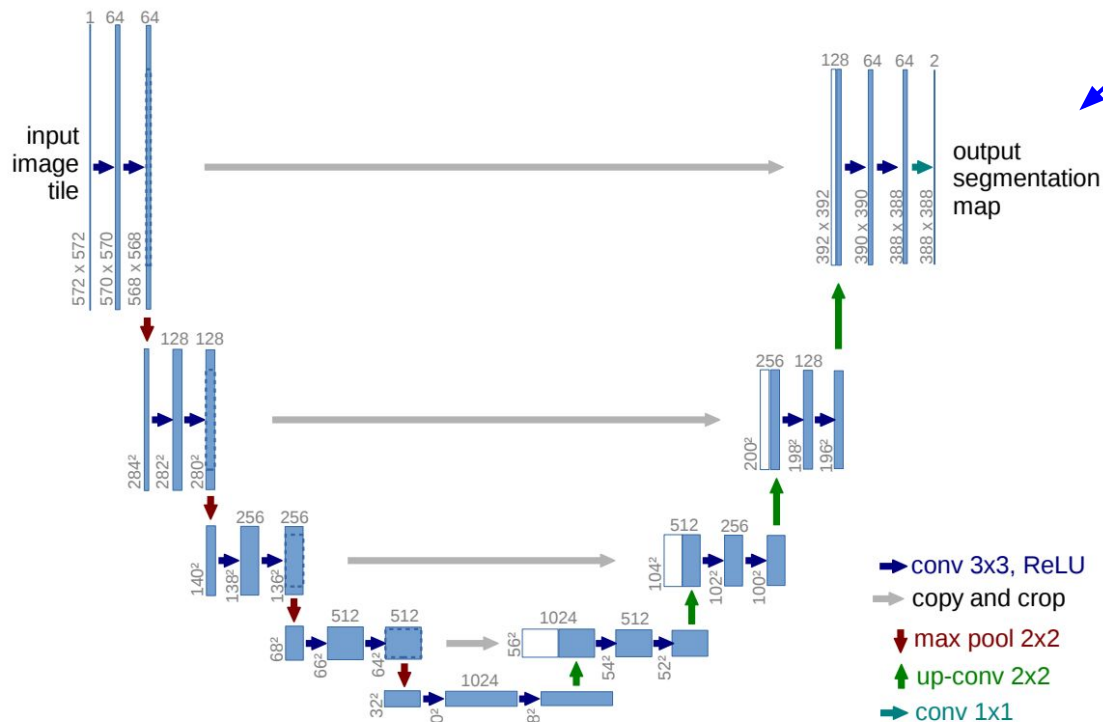
Output is an image mask: width x height x # classes

Output image size somewhat smaller than original, due to convolutional operations w/o padding



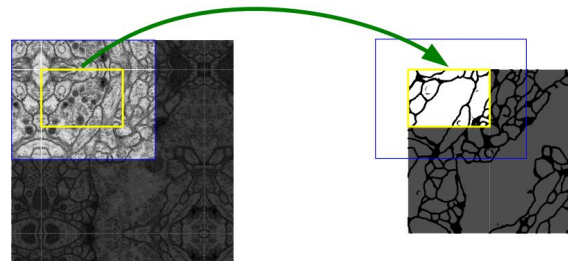
Ronneberger et al. 2015. U-Net: Convolutional Networks for Biomedical Image Segmentation. 2015.

Semantic segmentation: U-Net



Output is an image mask: width x height x # classes

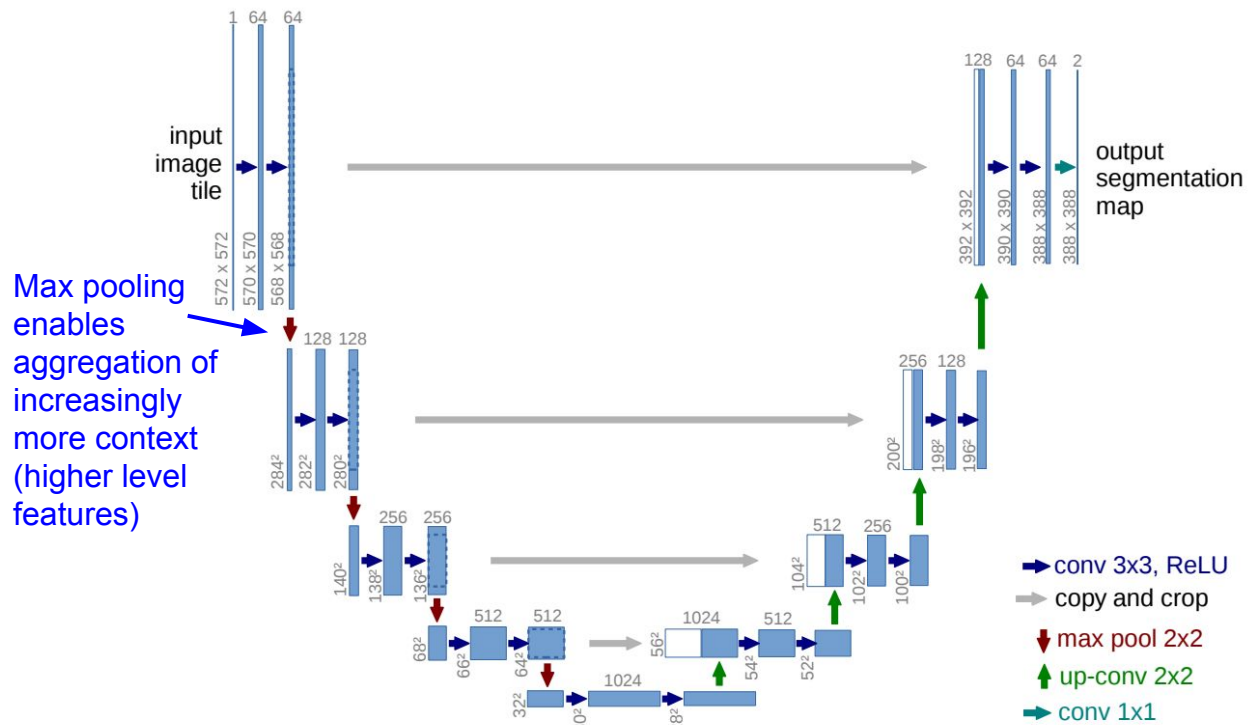
Output image size somewhat smaller than original, due to convolutional operations w/o padding



Gives more “true” context for reasoning over each image area. Can tile to make predictions for arbitrarily large images

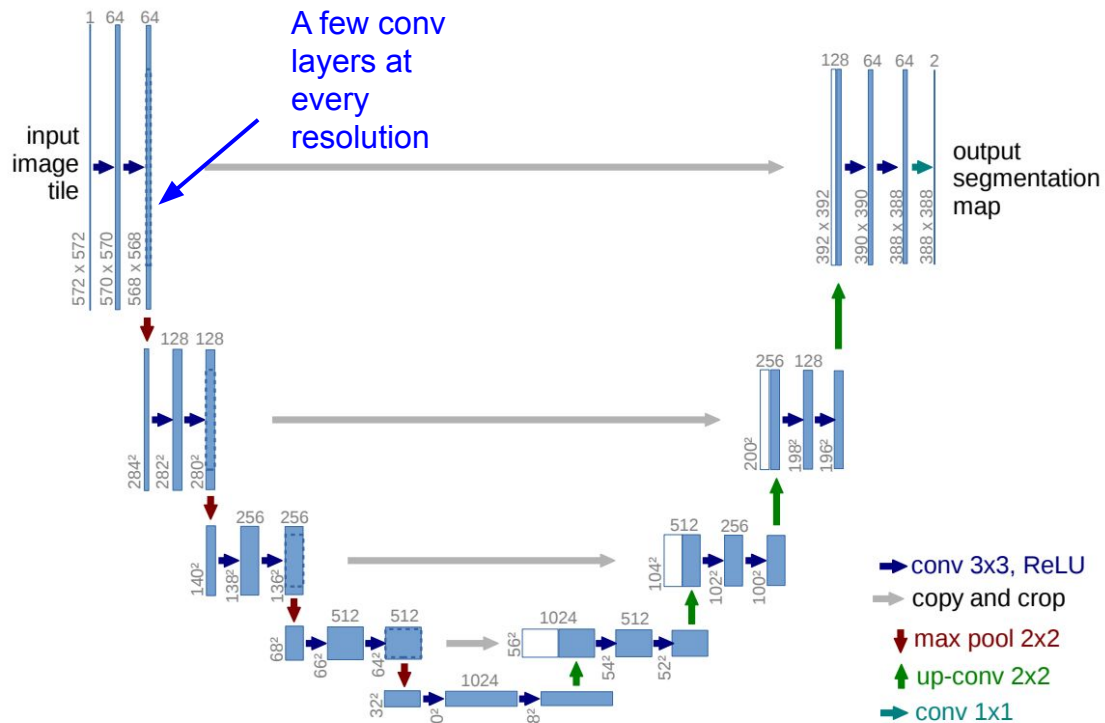
Ronneberger et al. 2015. U-Net: Convolutional Networks for Biomedical Image Segmentation. 2015.

Semantic segmentation: U-Net



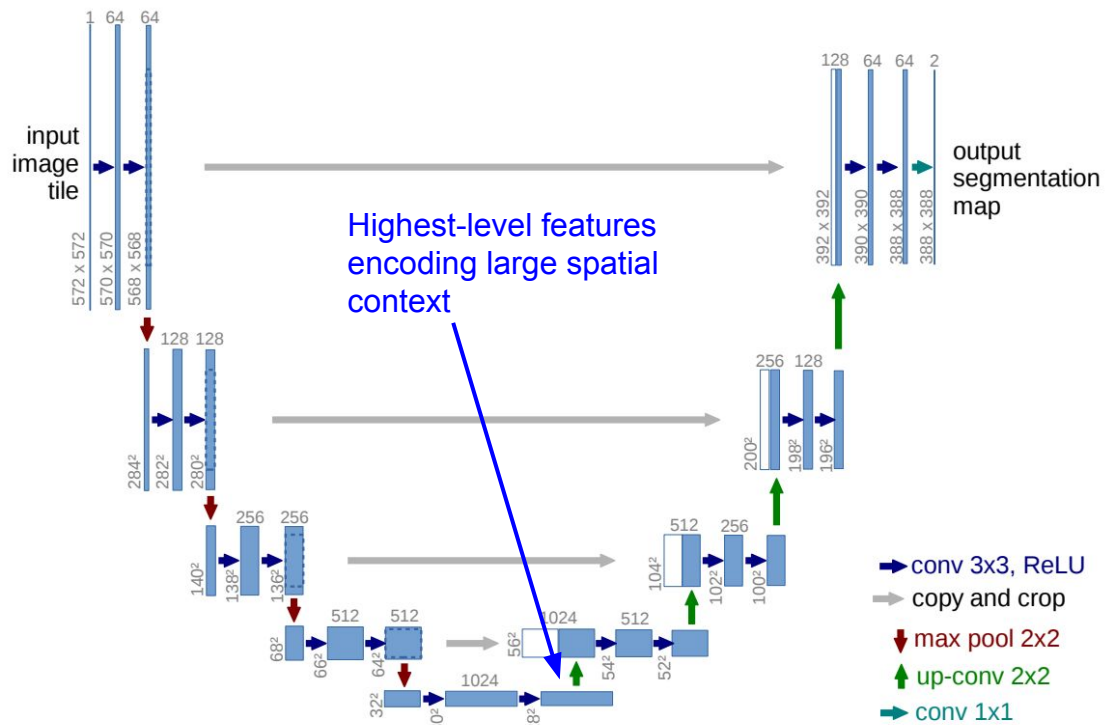
Ronneberger et al. 2015. U-Net: Convolutional Networks for Biomedical Image Segmentation. 2015.

Semantic segmentation: U-Net



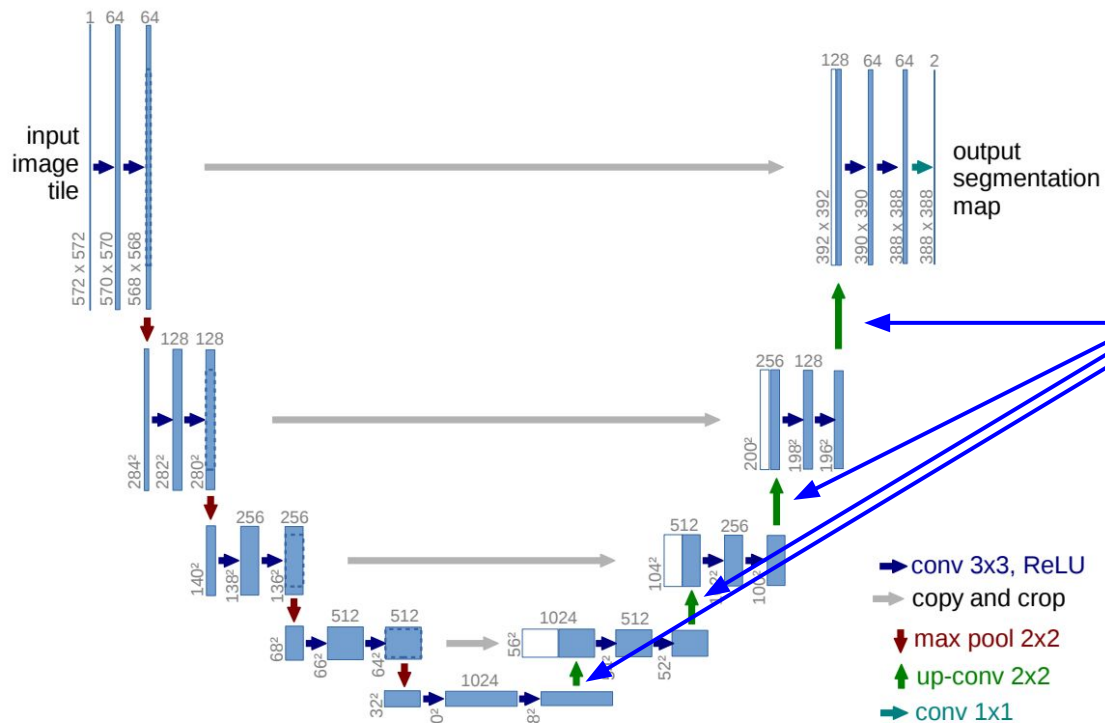
Ronneberger et al. 2015. U-Net: Convolutional Networks for Biomedical Image Segmentation. 2015.

Semantic segmentation: U-Net



Ronneberger et al. 2015. U-Net: Convolutional Networks for Biomedical Image Segmentation. 2015.

Semantic segmentation: U-Net

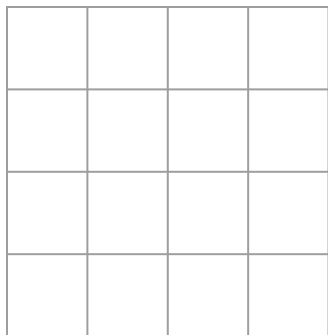


Up-convolutions to go from the global information encoded in highest-level features, back to individual pixel predictions

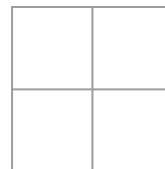
Ronneberger et al. 2015. U-Net: Convolutional Networks for Biomedical Image Segmentation. 2015.

Up-convolutions

Recall: Normal 3 x 3 convolution, stride 2 pad 1



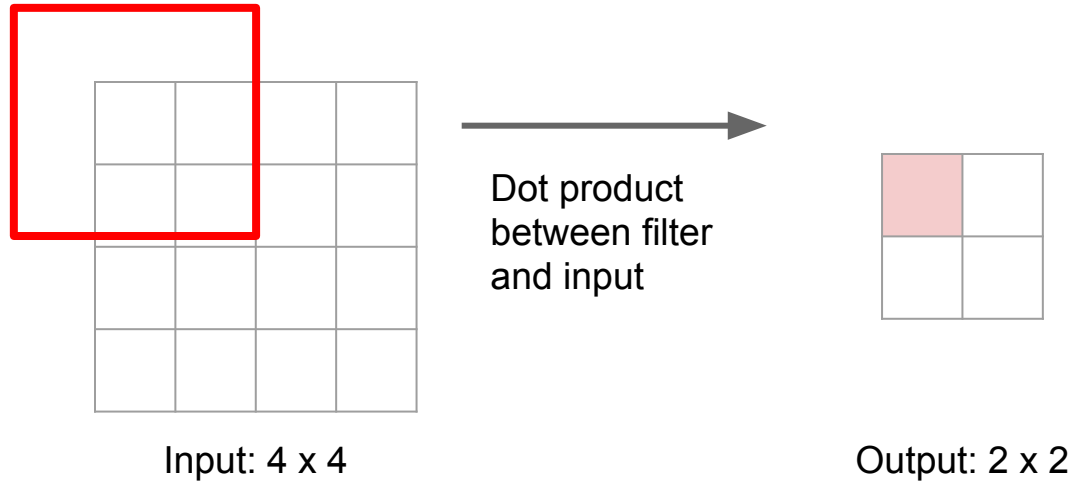
Input: 4 x 4



Output: 2 x 2

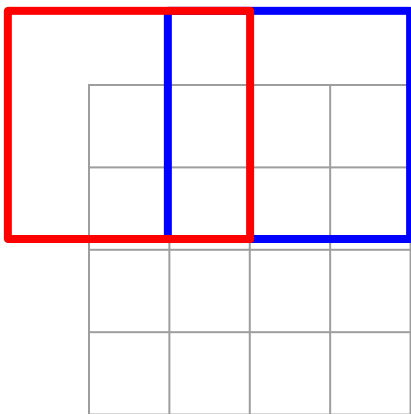
Up-convolutions

Recall: Normal 3 x 3 convolution, stride 2 pad 1



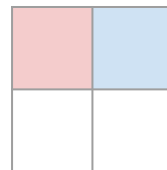
Up-convolutions

Recall: Normal 3 x 3 convolution, stride 2 pad 1



Input: 4 x 4

Dot product
between filter
and input



Output: 2 x 2

Filter moves 2 pixels in
the input for every one
pixel in the output

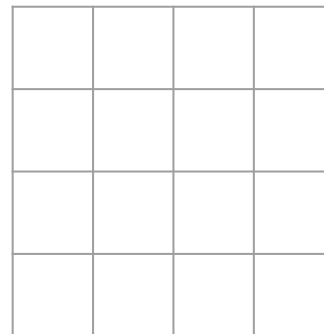
Stride gives ratio between
movement in input and
output

Up-convolutions

3 x 3 **transpose** convolution, stride 2 pad 1



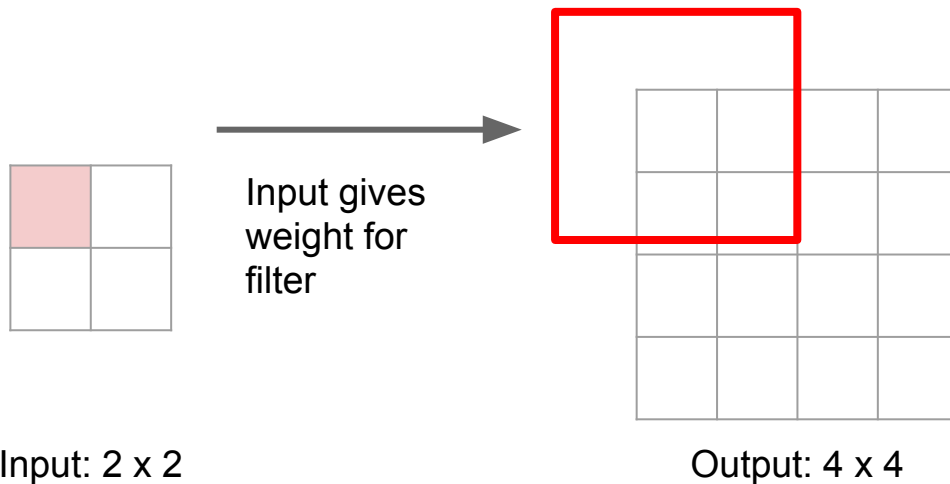
Input: 2 x 2



Output: 4 x 4

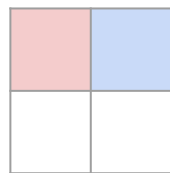
Up-convolutions

3 x 3 **up-convolution**, stride 2 pad 1



Up-convolutions

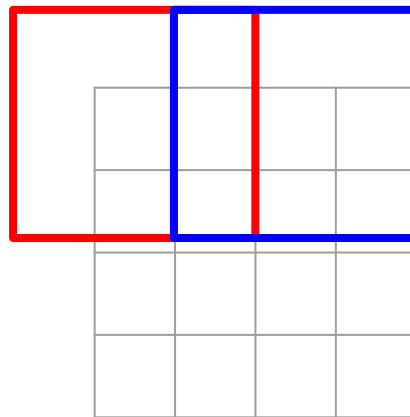
3 x 3 **up-convolution**, stride 2 pad 1



Input: 2 x 2



Input gives weight for filter



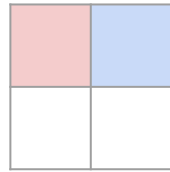
Output: 4 x 4

Filter moves 2 pixels in the output for every one pixel in the input

Stride gives ratio between movement in output and input

Up-convolutions

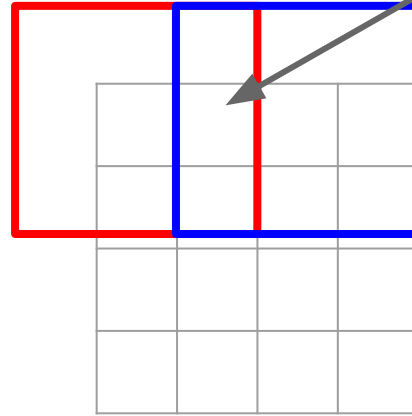
3 x 3 **up-convolution**, stride 2 pad 1



Input: 2 x 2



Input gives weight for filter



Output: 4 x 4

Sum where output overlaps

Filter moves 2 pixels in the output for every one pixel in the input

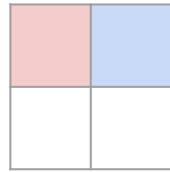
Stride gives ratio between movement in output and input

Up-convolutions

Other names:

- Transpose convolution
- Fractionally strided convolution
- Backward strided convolution

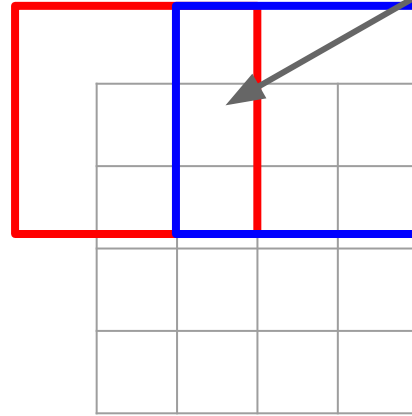
3 x 3 up-convolution, stride 2 pad 1



Input: 2 x 2



Input gives weight for filter



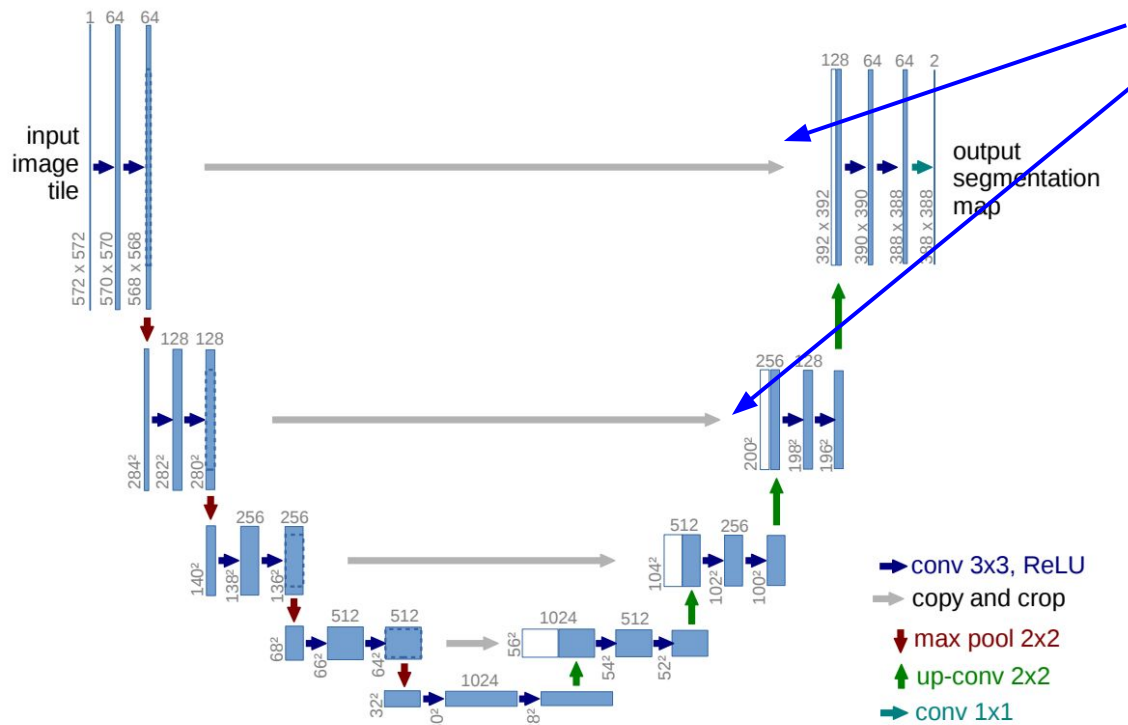
Output: 4 x 4

Sum where output overlaps

Filter moves 2 pixels in the output for every one pixel in the input

Stride gives ratio between movement in output and input

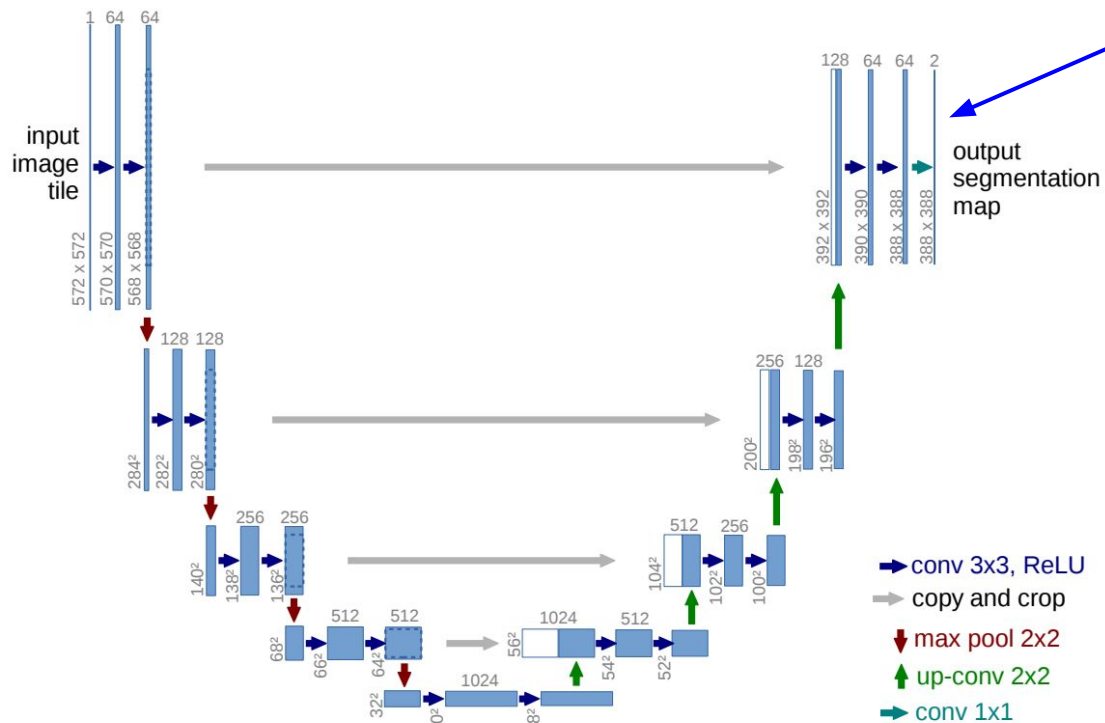
Semantic segmentation: U-Net



Concatenate with same-resolution feature map during downsampling process to combine high-level information with low-level (local) information

Ronneberger et al. 2015. U-Net: Convolutional Networks for Biomedical Image Segmentation. 2015.

Semantic segmentation: U-Net



Train with classification loss (e.g. binary cross entropy) on every pixel, sum over all pixels to get total loss

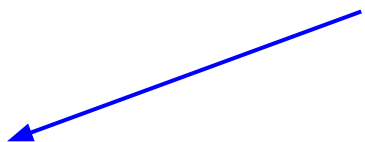
Ronneberger et al. 2015. U-Net: Convolutional Networks for Biomedical Image Segmentation. 2015.

Semantic segmentation: IOU evaluation

Intersection over Union:

$$IoU = \frac{target \cap prediction}{target \cup prediction}$$

pixels included in both
target and prediction
maps



Total # pixels in the
union of both masks

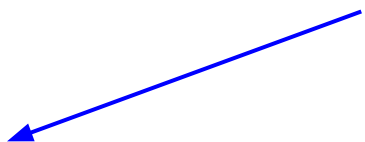


Semantic segmentation: IOU evaluation

Intersection over Union:

$$IoU = \frac{target \cap prediction}{target \cup prediction}$$

pixels included in both
target and prediction
maps



Total # pixels in the
union of both masks



Can compute this over all masks in the evaluation set, or at individual mask and image levels to get finer-grained understanding of performance.

Semantic segmentation: IOU evaluation

Intersection over Union:

$$IoU = \frac{target \cap prediction}{target \cup prediction}$$

pixels included in both
target and prediction
maps

Total # pixels in the
union of both masks

Can compute this over all masks in the evaluation set, or at individual mask and image levels to get finer-grained understanding of performance.

Also known as Jaccard
Index

Semantic segmentation: Pixel Accuracy evaluation

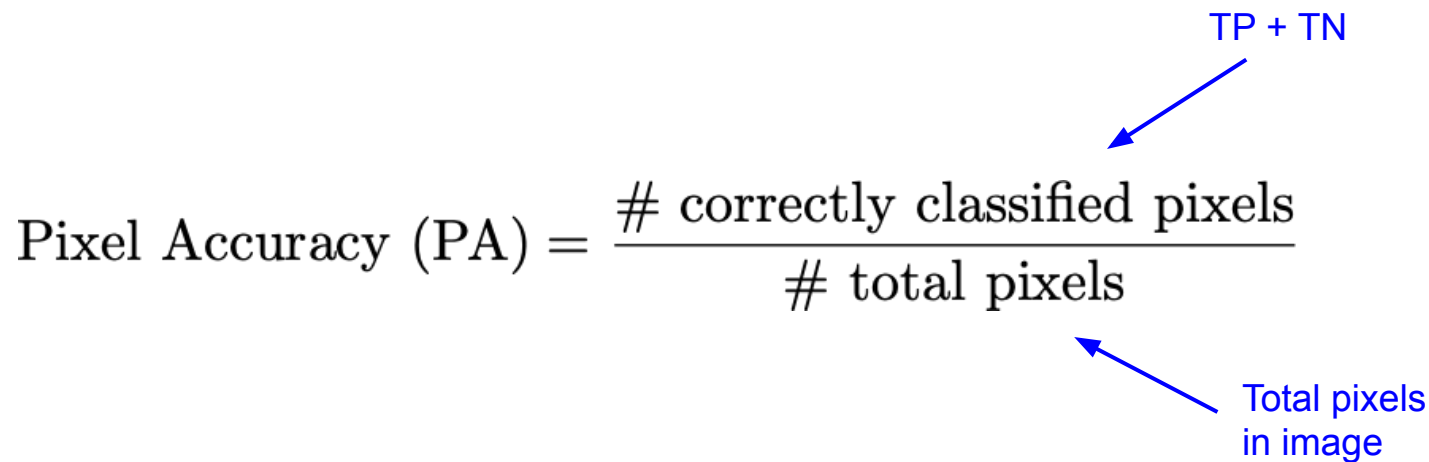
$$\text{Pixel Accuracy (PA)} = \frac{\# \text{ correctly classified pixels}}{\# \text{ total pixels}}$$

Semantic segmentation: Pixel Accuracy evaluation

$$\text{Pixel Accuracy (PA)} = \frac{\text{\# correctly classified pixels}}{\text{\# total pixels}}$$

TP + TN

Total pixels in image

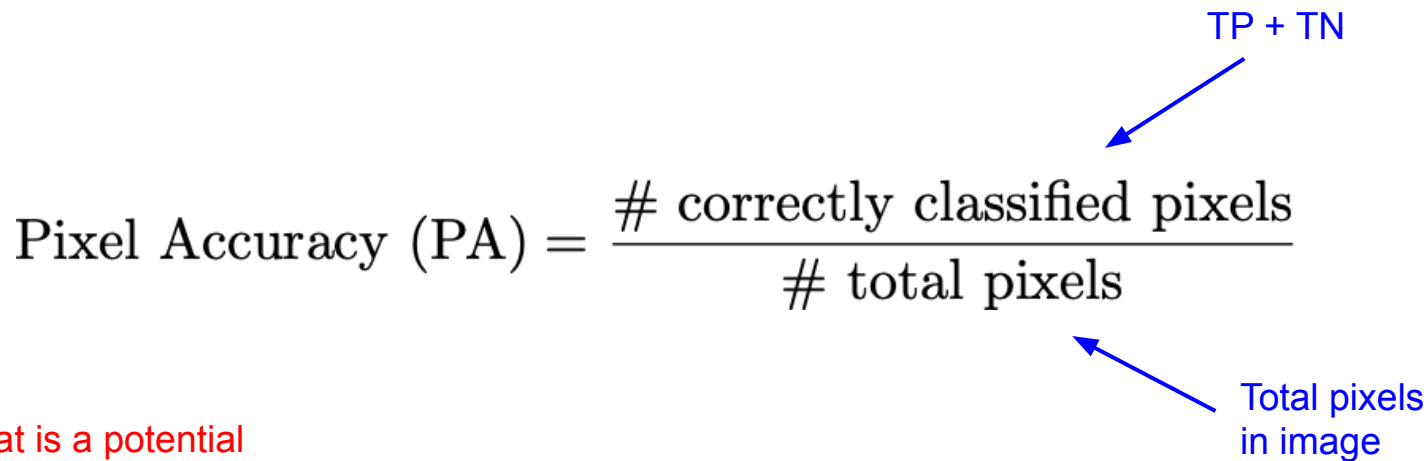
The diagram shows the formula for Pixel Accuracy (PA) as a fraction. The numerator is '# correctly classified pixels' and the denominator is '# total pixels'. A blue arrow points from the text 'TP + TN' to the numerator. Another blue arrow points from the text 'Total pixels in image' to the denominator.

Semantic segmentation: Pixel Accuracy evaluation

$$\text{Pixel Accuracy (PA)} = \frac{\text{\# correctly classified pixels}}{\text{\# total pixels}}$$

TP + TN

Total pixels in image



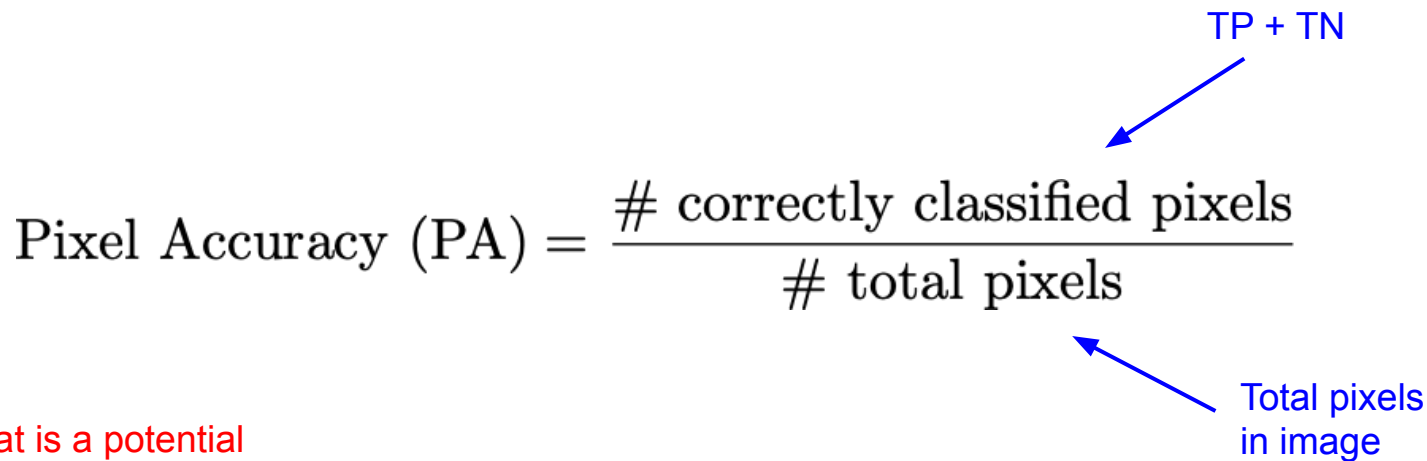
Q: What is a potential problem with this?

Semantic segmentation: Pixel Accuracy evaluation

$$\text{Pixel Accuracy (PA)} = \frac{\text{\# correctly classified pixels}}{\text{\# total pixels}}$$

TP + TN

Total pixels in image



Q: What is a potential problem with this?

A: Think about what happens when there is class imbalance.

Semantic segmentation: Dice coefficient evaluation

$$\text{Dice Coefficient} = \frac{2 * (\text{target} \cap \text{prediction})}{\# \text{ target mask pixels} + \# \text{ prediction mask pixels}}$$

Semantic segmentation: Dice coefficient evaluation

$$\text{Dice Coefficient} = \frac{2 * (\text{target} \cap \text{prediction})}{\# \text{ target mask pixels} + \# \text{ prediction mask pixels}}$$

2 * intersection

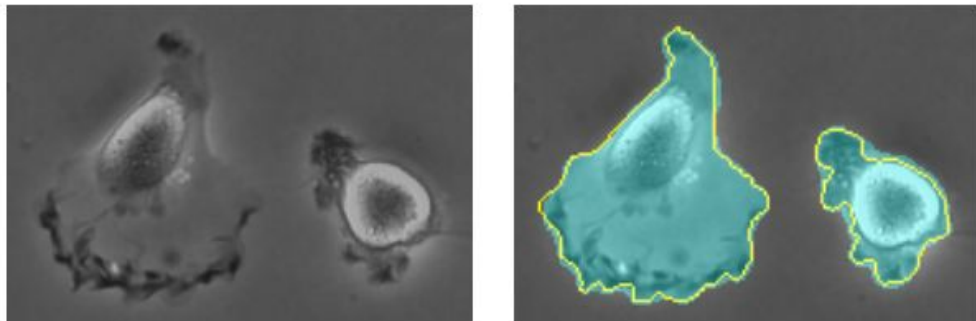
Sum of target mask size + prediction mask size

Very similar to IOU /
Jaccard, can derive one
from the other

Semantic segmentation: summary of evaluation metrics

- Most commonly use IOU / Jaccard or Dice Coefficient
- Sometimes will also see pixel accuracy
- If multi-class segmentation task, typically report all these metrics per-class, and then a mean over all classes

Semantic segmentation: U-Net cell segmentation

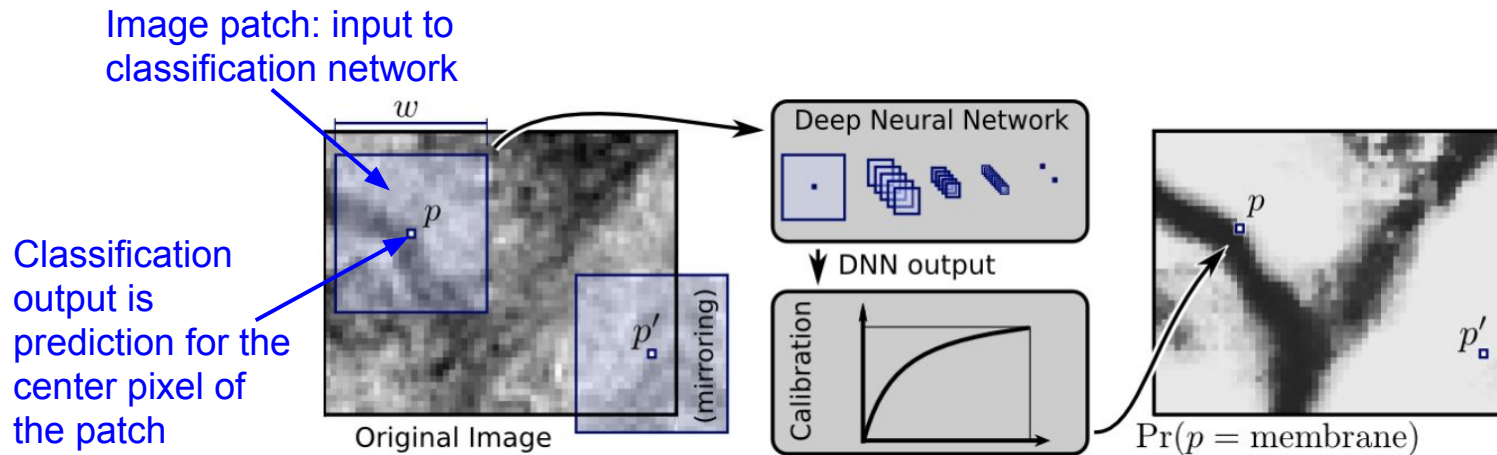


Name	PhC-U373	DIC-HeLa
IMCB-SG (2014)	0.2669	0.2935
KTH-SE (2014)	0.7953	0.4607
HOUS-US (2014)	0.5323	-
second-best 2015	0.83	0.46
u-net (2015)	0.9203	0.7756

Very small dataset: 30 training images of size 512x512, in the ISBI 2012 Electron Microscopy (EM) segmentation challenge. Used excessive data augmentation to compensate.

Ronneberger et al. U-Net: Convolutional Networks for Biomedical Image Segmentation. 2015.

Aside: segmentation through sliding-window pixel classification

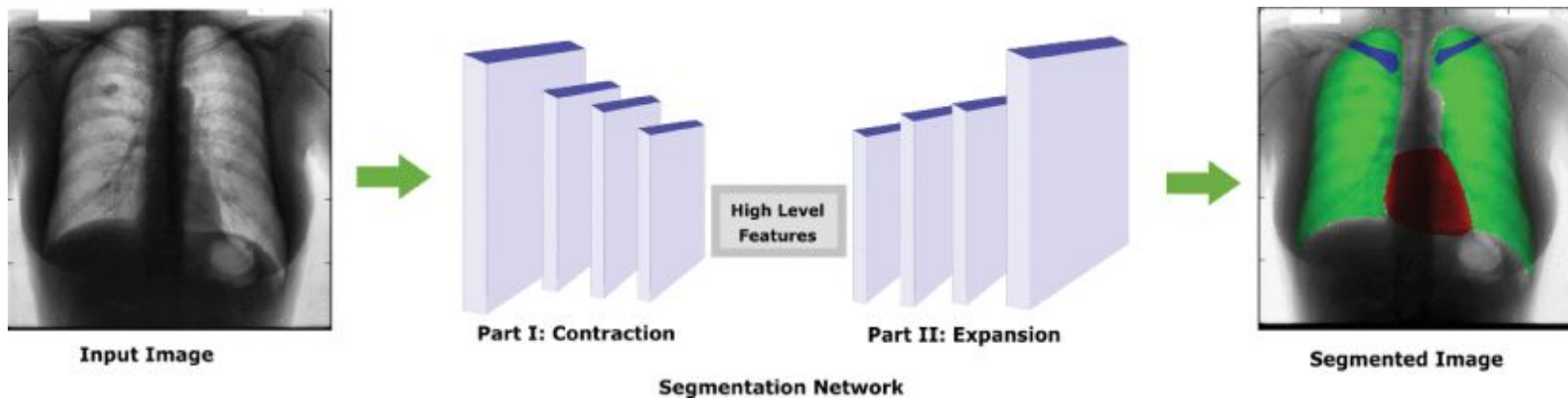


Note: a simple approach to segmentation can also be applying a classification CNN on image patches in a dense, sliding-window fashion (e.g. Ciaran et al.). But fully convolutional approaches such as U-Net generally achieve better performance.

Ciaran et al. Deep Neural Networks Segment Neuronal Membranes in Electron Microscopy Images. NeurIPS, 2012.

Novikov et al. 2018

- Chest x-ray segmentation of lungs, clavicles, and heart
- JSRT dataset of 247 chest-xrays at 2048x2048 resolution. (But downsampled to 128x128 and 256x256!)
- Used a U-Net based segmentation network with a few modifications

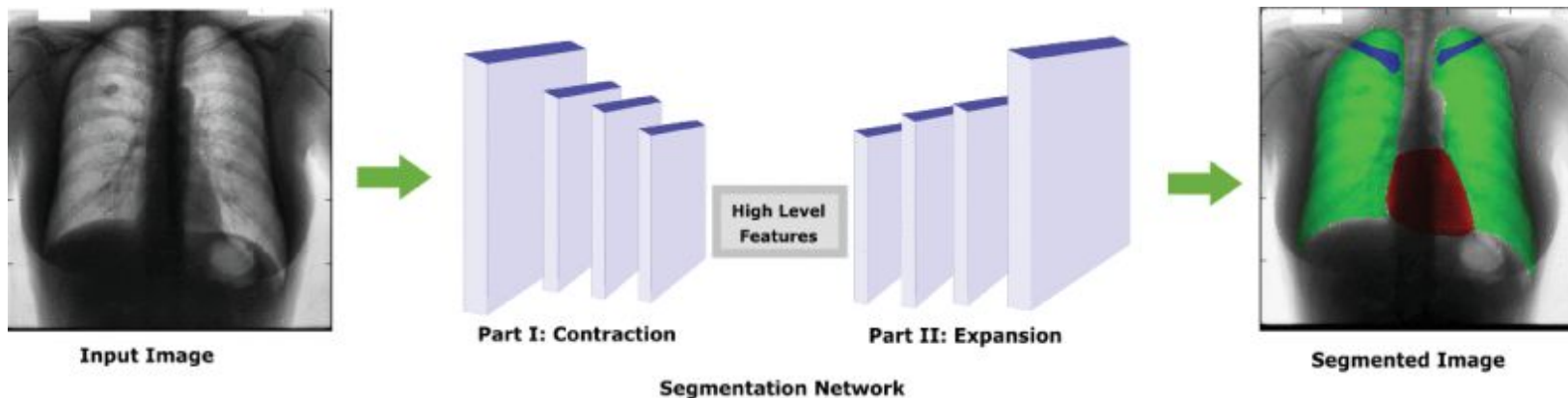


Novikov et al. Fully Convolutional Architectures for Multiclass Segmentation in Chest Radiographs. IEEE Trans. on Medical Imaging, 2018.

Novikov et al. 2018

Q: What loss function would be appropriate here?

- Chest x-ray segmentation of lungs, clavicles, and heart
- JSRT dataset of 247 chest-xrays at 2048x2048 resolution. (But downsampled to 128x128 and 256x256!)
- Used a U-Net based segmentation network with a few modifications



Novikov et al. Fully Convolutional Architectures for Multiclass Segmentation in Chest Radiographs. IEEE Trans. on Medical Imaging, 2018.

Novikov et al. 2018

- Multi-class segmentation -> tried both a per-pixel softmax loss as well as a loss based on the Dice coefficient.
- Class imbalance -> weight loss terms corresponding to each ground-truth class by inverse of class frequency: $(\# \text{ class pixels}) / (\text{total } \# \text{ pixels in data})$

Body Part	Lungs		Clavicles		Heart	
Evaluation Metric	<i>D</i>	<i>J</i>	<i>D</i>	<i>J</i>	<i>D</i>	<i>J</i>
InvertedNet	0.972	0.946	0.902	0.821	0.935	0.879
All-Dropout	0.973	0.948	0.896	0.812	0.941	0.888
All-Convolutional	0.971	0.944	0.876	0.780	0.938	0.883
Original U-Net	0.971	0.944	0.880	0.785	0.938	0.883

Novikov et al. Fully Convolutional Architectures for Multiclass Segmentation in Chest Radiographs. IEEE Trans. on Medical Imaging, 2018.

Image ground truth class mask

$$L_{\text{dice}}(y, \hat{y}) = 1 - \frac{2 \sum_{i,j} y_{i,j} \hat{y}_{i,j}}{\sum_{i,j} y_{i,j} + \sum_{i,j} \hat{y}_{i,j}}$$

Image pixel class probabilities

Novikov et al. 2018

- Multi-class segmentation -> tried both a per-pixel softmax loss as well as a loss based on the Dice coefficient. **Note: this Dice loss is often useful to try!**
- Class imbalance -> weight loss terms corresponding to each ground-truth class by inverse of class frequency: (# class pixels) / (total # pixels in data)

Body Part	Lungs		Clavicles		Heart	
Evaluation Metric	<i>D</i>	<i>J</i>	<i>D</i>	<i>J</i>	<i>D</i>	<i>J</i>
InvertedNet	0.972	0.946	0.902	0.821	0.935	0.879
All-Dropout	0.973	0.948	0.896	0.812	0.941	0.888
All-Convolutional	0.971	0.944	0.876	0.780	0.938	0.883
Original U-Net	0.971	0.944	0.880	0.785	0.938	0.883

Novikov et al. Fully Convolutional Architectures for Multiclass Segmentation in Chest Radiographs. IEEE Trans. on Medical Imaging, 2018.

Novikov et al. 2018

Image ground truth class mask

$$L_{\text{dice}}(y, \hat{y}) = 1 - \frac{2 \sum_{i,j} y_{i,j} \hat{y}_{i,j}}{\sum_{i,j} y_{i,j} + \sum_{i,j} \hat{y}_{i,j}}$$

Image pixel class probabilities

- Multi-class segmentation -> tried both a per-pixel softmax loss as well as a loss based on the Dice coefficient. **Note: this Dice loss is often useful to try!**
- Class imbalance -> weight loss terms corresponding to each ground-truth class by inverse of class frequency: (# class pixels) / (total # pixels in data)

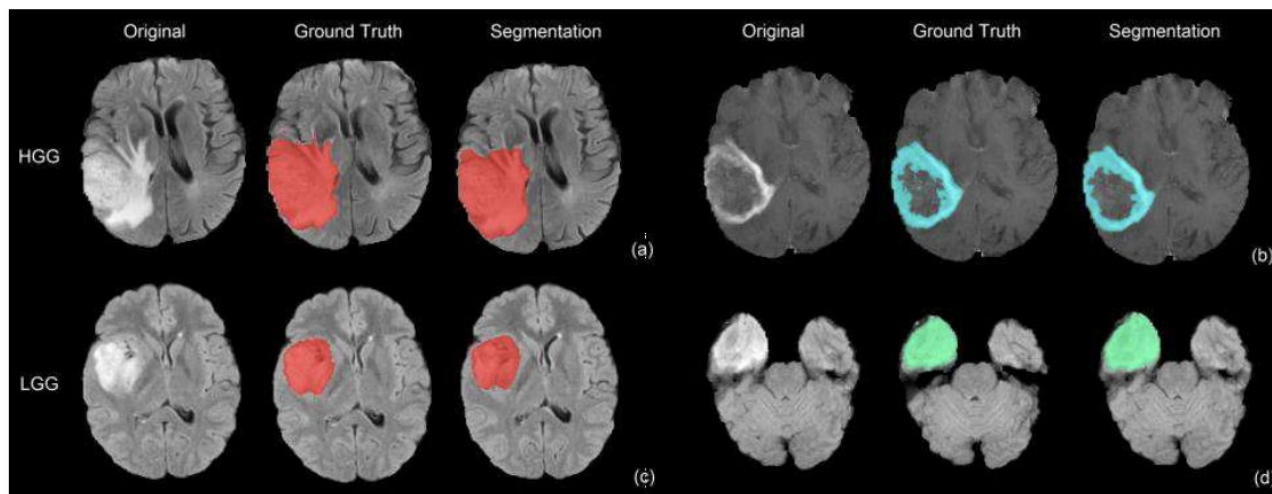
Body Part	Lungs		Clavicles		Heart	
Evaluation Metric	<i>D</i>	<i>J</i>	<i>D</i>	<i>J</i>	<i>D</i>	<i>J</i>
InvertedNet	0.972	0.946	0.902	0.821	0.935	0.879
All-Dropout	0.973	0.948	0.896	0.812	0.941	0.888
All-Convolutional	0.971	0.944	0.876	0.780	0.938	0.883
Original U-Net	0.971	0.944	0.880	0.785	0.938	0.883

Dice and Jaccard evaluation

Novikov et al. Fully Convolutional Architectures for Multiclass Segmentation in Chest Radiographs. IEEE Trans. on Medical Imaging, 2018.

Dong et al. 2017

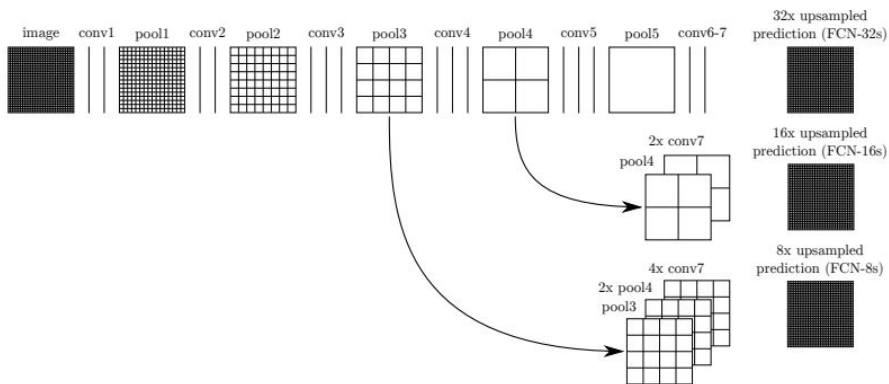
- Segmentation of tumors in brain MR image slices
- BRATS 2015 dataset: 220 high-grade brain tumor and 54 low-grade brain tumor MRIs
- U-Net architecture, Dice loss function



Dong et al. Automatic Brain Tumor Detection and Segmentation Using U-Net Based Fully Convolutional Networks. MIUA, 2017.

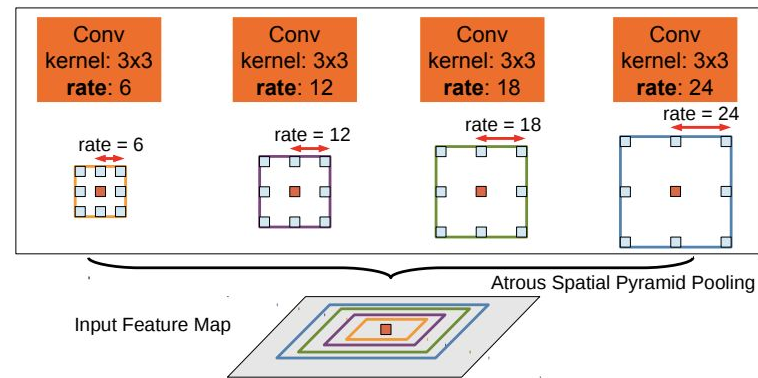
Other segmentation architectures

- **Fully convolutional networks (FCN)**
- Pre-cursor to U-Net, similar in structure but simpler upsampling pathway



Shelhamer*, Long*, et al. Fully Convolutional Networks for Semantic Segmentation. CVPR 2015.

- **DeepLab (v1-v3)**
- Uses “atrous convolutions” to control a filter’s field of view
- Parallel atrous convolutions with different rates for multi-scale features



Chen et al. DeepLab: Semantic Image Segmentation with Deep Convolutional Nets, Atrous Convolution, and Fully Connected CRFs. IEEE TPAMI, 2017.

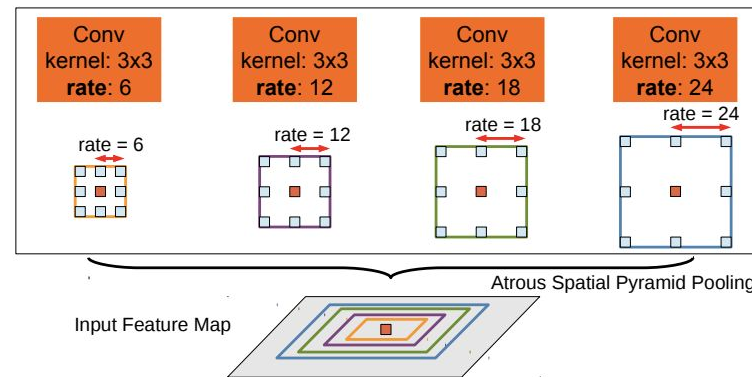
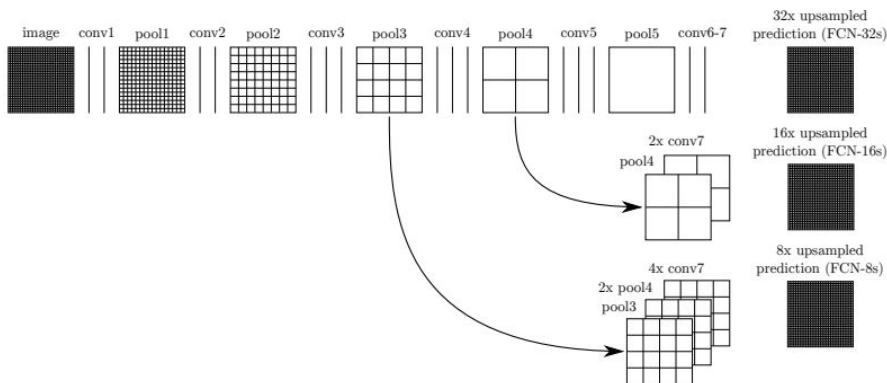
Chen et al. Rethinking Atrous Convolution for Semantic Image Segmentation. 2917.

Other segmentation architectures

Can try DeepLab v3+ for segmentation projects!

- Fully convolutional networks (FCN)
- Pre-cursor to U-Net, similar in structure but simpler upsampling pathway

- DeepLab (v1-v3+)
- Uses “atrous convolutions” to control a filter’s field of view
- Parallel atrous convolutions with different rates for multi-scale features



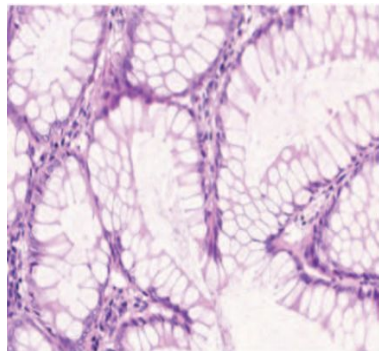
Shelhamer*, Long*, et al. Fully Convolutional Networks for Semantic Segmentation. CVPR 2015.

Chen et al. DeepLab: Semantic Image Segmentation with Deep Convolutional Nets, Atrous Convolution, and Fully Connected CRFs. IEEE TPAMI, 2017.

Chen et al. Rethinking Atrous Convolution for Semantic Image Segmentation. 2917.

Richer visual recognition tasks: segmentation and detection

Classification



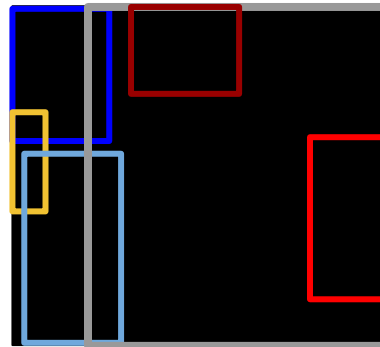
Output:
one category label for
image (e.g., colorectal
glands)

Semantic Segmentation



Output:
category label for each pixel
in the image

Detection



Output:
Spatial bounding box for
each **instance** of a
category object in the
image

Instance Segmentation

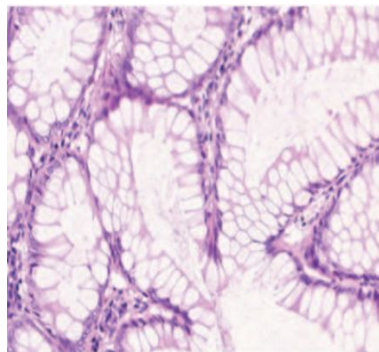


Output:
Category label and instance
label for each pixel in the
image

Figures: Chen et al. 2016. <https://arxiv.org/pdf/1604.02677.pdf>

Richer visual recognition tasks: segmentation and detection

Classification



Output:
one category label for
image (e.g., colorectal
glands)

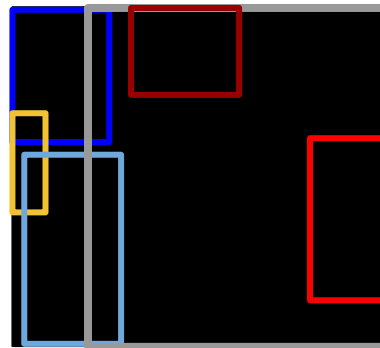
Semantic Segmentation



Output:
category label for each pixel
in the image

Next Time:

Detection



Output:
Spatial bounding box for
each **instance** of a
category object in the
image

Instance Segmentation



Output:
Category label and instance
label for each pixel in the
image

Distinguishes between different instances of an object

Summary

Finished up medical image classification

Beyond classification to richer visual recognition tasks

- Semantic segmentation
- Object detection
- Instance segmentation

Next time: Advanced vision models (Object detection, Instance segmentation, 3D and video)